Weather and Climate Extremes 40 (2023) 100554

Contents lists available at ScienceDirect

Weather and Climate Extremes

journal homepage: www.elsevier.com/locate/wace

# Long-term trend analysis of extreme climate in Sarawak tropical peatland under the influence of climate change

Zulfaqar Sa'adi [a,**], Zaher Mundher Yaseen [b,c,*], Aitazaz Ahsan Farooque [d,e], Nur Athirah Mohamad [f], Mohd Khairul Idlan Muhammad [f], Zafar Iqbal [g,h]

[a] Centre for Environmental Sustainability and Water Security (IPASA), School of Civil Engineering, Faculty of Engineering, Universiti Teknologi Malaysia, 81310 UTM, Sekudai, Johor, Malaysia
[b] Civil and Environmental Engineering Department, King Fahd University of Petroleum & Minerals, Dhahran 31261, Saudi Arabia
[c] Interdisciplinary Research Center for Membranes and Water Security, King Fahd University of Petroleum & Minerals, Dhahran 31261, Saudi Arabia
[d] Canadian Center for Climate Change and Adaptation University of Prince Edward Island, St Peter's Bay, PE, Canada
[e] Faculty of Sustainable Design Engineering, University of Prince Edward Island, Charlottetown, PE C1A4P3, Canada
[f] Department of Water and Environmental Engineering, Faculty of Civil Engineering, Universiti Teknologi Malaysia (UTM), 81310 Johor Bahru, Malaysia
[g] NUST Institute of Civil Engineering-SCEE, National University of Sciences and Technology (NUST), H-12, Islamabad, 44000, Pakistan
[h] New Era and Development in Civil Engineering Research Group, Scientific Research Center, Al-Ayen University, Thi-Qar, 64001, Iraq

ARTICLE INFO

*Keywords:*
Climate extremes
Mann-Kendall test
Modified Mann-Kendall test
Sarawak
Tropical peatland

ABSTRACT

Extreme climate is one of the important variables which determine the capability of tropical peatland to act as either carbon sink and/or carbon source. The purpose of this study is to reveal the spatio-temporal trend in the long-term time series of extreme rainfall and temperature in Sarawak peatland cause by climate change. Gridded-based Princeton datasets were used for trend analysis spanning 68-year (1948–2016) based on Modified Mann-Kendall (m-MK) test which has the capability of distinguishing unidirectional trend with multi-scale variability. The m-MK test was also used to confirm the increasing or decreasing trend produce by Mann-Kendall (MK), and to discriminate the exaggeration in trend caused by serial auto-correlation due to the high effect of large scale climate events regulating the climate in the region. By using R-based program, RClimDex for extreme climate indices output, extreme climate under Northeast (NE) and Southwest (SW) monsoon showed lower grid point with significant changes under m-MK test compared to MK test at 95% significance level. Here, the exaggeration of trend by MK test has been reduced by using m-MK test which can accommodate the scaling effect in the time series due to inherent natural climate variability. Diurnal temperature range (DTR) was expected to decrease for both monsoons in the central-coastal region as minimum temperature (TN) increased more than maximum temperature (TX). Significant increase in extreme rainfall (R10, R20, Rnn) was spatially observed more during SW monsoon compared to NE monsoon, although with high spatial variability. Significant increase of TN indices of TNn and TN90p might cause increased rainfall intensity in the south and central-coastal region, while high TX indices of TXn might cause increased rainfall intensity in the north. Due to the imminent threat of climate change, this study gives scientists an essential view on the behavior of different extreme climate variables and its potential impact on the peatland area which is susceptible to flood and risk of fire during the NE and SW monsoon, respectively.

## 1. Introduction

The hydrological cycle has been drastically affected by the increase in global temperature and has consequently brought about increases in the rates of rainfall and temperature (Beyaztas and Yaseen, 2019; Warburton et al., 2010). These changes in the rates of temperature and rainfall have further increased the extent and magnitude of climatic changes globally (Khan et al., 2018; Pour et al., 2020; Yaseen et al.,

* Corresponding author. Civil and Environmental Engineering Department, King Fahd University of Petroleum & Minerals, Dhahran 31261, Saudi Arabia.
** Corresponding author.
*E-mail addresses:* zulfaqar@utm.my (Z. Sa'adi), z.yaseen@kfupm.edu.sa (Z.M. Yaseen), afarooque@upei.ca (A.A. Farooque), nathirah75@live.utm.my (N.A. Mohamad), mohdkhairulidlan@utm.my (M.K.I. Muhammad), zafar.thalvi@gmail.com (Z. Iqbal).

https://doi.org/10.1016/j.wace.2023.100554
Received 9 December 2021; Received in revised form 28 December 2022; Accepted 14 February 2023
Available online 18 February 2023

2021). According to the Intergovernmental Panel on Climate Change (IPCC), owing to the sensitivity of the ecology of the tropical region to insignificant changes in climate characteristics, such region is normally considered more susceptible to changes in climate (IPCC, 2014; Mishra and Liu, 2014; Yang et al., 2005). For instance, most coastline tropical countries have witnessed significant changes climatic pattern over the years (Mayowa et al., 2015; Sa'adi et al., 2017); the study by Mayowa et al. (2015) observed substantial changes in the annual and seasonal rainfall and days of rainfall in the east coast of Peninsular Malaysia. Furthermore, significant changes in annual maximum rainfall has been witnessed across Sarawak which suggests a high impact of climatic variability across the region (Halder et al., 2021; Sa'adi et al., 2017).

Under such vulnerability, the eco-environmental systems in tropical regions, particularly the State of Sarawak located in the north-western region in the island of Borneo may become more susceptible to the changes in the climate (Mishra and Liu, 2014). Tropical peatland characterized with a deep peat profile plays an essential role in sequestering and storing more than 70 Gt (20% of global peatland carbon) carbon in peat domes. The carbon storage has been preserved for thousands of years by waterlogging, which suppresses decomposition (Cobb et al., 2017). Water table in tropical peatland is generally high because it lies mostly in coastal, low-lying regions, and high annual rainfall. The water table gradient is small with very high permeability of the surface layer, consist of a mixed of woody debris, leaves, and peaty material, as the water flows slowly into the bounding rivers (Cobb and Harvey, 2019; Dommain et al., 2015). The high water table and high permeability of the surface layer in the natural peat condition, allow the accumulation rate of the organic material to surpass the decomposition rate. In addition, high heterogeneity of hydraulic properties in the vertical and horizontal direction characterize how the change in water table govern the storage of the catchment (Cobb and Harvey, 2019). Therefore, any changes affecting the tropical peatland will change its capability to act as a sink of greenhouse gases (GHG).

Various studies have shown that human activities by fire and drainage through the conversion of pristine tropical peatland into various types of land use has altered its function as carbon sink (Cobb et al., 2017). However, there is a lack of knowledge on how climatic drivers due to the changing global climate might affect the function of the tropical peatland ecosystem. Within the context of climate change, a clear insight on the biological and environmental effect of climatic drivers is crucial, because it provides a basis for anticipating and preparing for the effects of future change (Alamgir et al., 2020; Halder et al., 2022).

Extreme climate events may cause a major impact on peatland environment as it exerts more immediate and profound effects due to high sensitivity of peat with the changing climate (Behnke et al., 2016; Ise et al., 2008). However, insufficient information was known regarding trends in extreme climate in relation with Sarawak peatland. This is due to difficult passage into typically inundated peatland environments, causing a lack of meteorological stations to cover a wide range of peat area. Poor accessibility subsequently causes poor availability of climate data, quality and its dependability. The number of rainfall days and warm nights in Kuching station has been found to increase significantly by Manton et al. (2001) in response to the extent of decline in the number of cool nights and days. Sa'adi et al. (2017) reported a significant trend of 6- and 72-h maximum rainfall at the Lower Rajang basin (peatland area). This area is highly prone to extreme climate as it is exposed to various type of climate events. For instance, the climate-induced extended droughts (El Niño) and excessive rainfall rates (La Niña) could significantly affect vegetation structure and richness in peatland areas (Dohong et al., 2017). The prolonged drought associated with the El Niño events could significantly affect the groundwater table, and this could lead to improved peat oxidation, microbial activities, and consequently increase $CO_2$ emission. In recent years, forest fires have been a common event in the Borneo, Sumatra, Peninsular Malaysia, and West Papua with the most severe events been associated with the El Niño phase of El Niño-Southern Oscillation (ENSO) that prolonged the drought periods (Miettinen et al., 2017; Najib et al., 2022; Tu et al., 2016). Coastal peatland in low-lying areas make it vulnerable to flood and on the contrary, prone to fires during the relatively dry period due to the carbon rich ecosystem. Any variation in the rate of extreme climate recurrence or severity, could have profound impacts on the peatland as it affects the fluctuation of the water tables and subsequently its capability for carbon accumulation and storage (Hikouei et al., 2023; Mezbahuddin et al., 2022).

Most of the long-term global climate studies do not highlight the changes in extreme value (Manton et al., 2001; Salman et al., 2021; Zhang et al., 2005). This is due to the scarcity of climate data with high quality that was required for identification, detection and monitoring for changes in extreme climate. High quality data was required, as the occurrence of extreme events may be overlooked even with a smaller extent of missing data. Without proper assessment, complication may increase due to invalid data where outliers can be mistakenly thought as true data and vice versa. Climate data are prone to discontinuities and inhomogeneities as a result of the station set-up, location, and natural exposure; it could also be attributed to variations in observational procedure (Manton et al., 2001). The problem is compounded by sparse meteorological stations and their heterogeneous distribution when studying the large-scale spatial pattern of the extreme climate. Besides, extreme events tend to be more localized which can only be captured over a small and sufficient spatial and temporal resolution. Extreme events are also sensitive to spatial heterogeneity where nonlinear responses may be observed.

Such limitations make spatio-temporally constant yet fine-resolution gridded climate data more appropriate for the extreme climate assessment within inaccessible peatland areas. Examples of gridded-based climate data are Global Meteorological Forcing Dataset for land surface modelling by Land Surface Hydrology Research Group, Princeton University (Princeton) (Sheffield et al., 2006), Global Precipitation Climatology Centre (GPCC) (Schnider et al., 2011), Climatic Research Unit (CRU) (Harris et al., 2013), Asian Precipitation-Highly-Resolved Observational Data Integration Towards Evaluation (APHRODITE) (Yatagai et al., 2009), University of Delaware (UDel) (Matsuura and Willmott, 2012), Tropical Rainfall Measuring Mission (TRMM) (Huffman et al., 2015), ECMWF Re-Analysis (ERA) (Decker et al., 2012) and Modern-Era Retrospective analysis for Research and Applications (MERRA) (Rienecker et al., 2011). Numbers of studies have applied gridded-based climate datasets for climate trend analysis (Agnihotri et al., 2018; Asfaw et al., 2018; Khan et al., 2018; Nashwan and Shahid, 2019). Therefore, a more specific study on extreme climate employing fine resolution climate data to capture climate extreme and its spatio-temporal pattern could be employed in Sarawak peatland. Hence, gridded-based Princeton (Sheffield et al., 2006) climate data sets was retrieved for this study to tailor for the demand for finer resolution of spatial and longer temporal climate information spanning 1948 to 2016. In addition, Princeton dataset can deliver near-surface meteorological data with the availability of the rainfall and temperature data for extreme climate trend analysis. It merges observations and reanalysis data which was then homogeneously disaggregated (temporally and spatially) based on bias-corrected climate model output. Previous works also have validated and utilized these datasets in the tropical climate countries for various purposes (Ang et al., 2022; Ayoub et al., 2020; Sa'adi et al., 2021; Singh and Xiaosheng, 2019).

There are many methods developed for calculating and monitoring extreme climate including a combination of indices by employing various type of input datasets (Adeyeri et al., 2022; He et al., 2017; Katsanos et al., 2018; Shamshirband et al., 2020; Sun et al., 2016; Zhao et al., 2018). For the purposes of defining meaningful extreme indices which are consistent across a wide region, Frich et al. (2002) created the Expert Team on Climate Change Detection and Indices (ETCCDI) to illustrate a wide range of climates indices and indicators. In total, 27 indices were defined and have been applied for climate extreme study in

various parts of the world (POPOV et al., 2017; Rahimi et al., 2018; Razavi et al., 2016). The ETCCDI indices let a direct monitoring of the intensity and frequency of climatic trend, which would possibly cause stress to human, biological condition or the environment. Other studies (Fung et al., 2022; Nashwan et al., 2019; Syafrina et al., 2017; Tan et al., 2021) investigated extreme climate trend and show a contrasting spatio-temporal results, mainly because of the usage of different definitions of extreme event (Lacombe and McCartney, 2014). Therefore, a generally adopted ETCCDI indices was employed in this study due to the comprehensive list of the indices being provided and its suitability to be employed in the tropical country as well as other countries for comparative assessment (Panda et al., 2016). The use of ETCCDI indices has been employed in other part of Malaysia (Hanif et al., 2022; Hasan et al., 2016; Ng et al., 2022), and indeed has accelerated further research into observed climate extremes, as well as further research into model simulation and assessment of such events (Yin and Sun, 2018).

A standard method of parametric/non-parametric trend analysis has been adopted in the past for climate trend assessment (Hanif et al., 2022; Kozan, 2020; Krishnan et al., 2018; Leong Tan et al., 2019). However, anthropogenic climate change forcing in trend assessment can be misguided due to the persistence of the internal variability of the natural climate (Armal et al., 2018). Therefore, several studies have been conducted to address this issue. Mallick et al. (2022) used trend free pre-whitening (TFPW) technique to eliminate serial autocorrelation before implementing the MK test in the assessment of temperature extremes in Bangladesh. Armal et al. (2018) use Bayesian multilevel model to identify the annual frequency of extreme rainfall events more accurately across the contiguous United States by pooling information across stations to minimize parameter estimation uncertainty. Panda et al. (2016) examine the heavy tails of the probability density function (PDF) among the pooled grid scale meteorological indices in different sub-periods to better diagnose the changes. Wang (2008) proposes an empirical approach incorporated in a stepwise testing algorithm to account for lag-1 autocorrelation in identifying mean shifts in time series to detect single or multiple changepoints It has been demonstrated that the new algorithms detect single or multiple changepoints in real-world climate data series very well and quickly. Lately, non-parametric MK test has been broadly applied for trend tests since it does not adopt an underlying probability distribution of the data time series and has low sensitivity to sudden disruptions due to data inhomogeneity (Shahid, 2010; Zhang et al., 2005). However, the output of the MK test can be exaggerated by serial auto-correlation triggering an increase in the chance for significance in trend (Zhang et al., 2005). MK test also sensitive with the long-term persistence (LTP) due to natural variability in the time series (Fathian et al., 2014; Lacombe et al., 2012; Shahid et al., 2014). By taking into account the LTP into the MK equation, Hamed (2008) has reported a substantial reduction in the significance of trends. Therefore, an iterative procedure which modified the MK method by Hamed (2008, 2009) to account for the scaling effect has gained its popularity due to its capability in distinguishing multi-scale variability of unidirectional trends for various climate indices.

In this paper, we present a spatio-temporally detailed long-term trend analysis spanning 68 years of extreme rainfall and temperature in Sarawak peatland based on m-MK to confirm the significance of the test output under MK. The m-MK test was employed to reveal the trend in the time series that is cause by climate change by discriminating the exaggeration in trend cause by serial auto-correlation due to the high influence of large scale climate phenomena governing the region. Previous studies only estimate the changes in climate trend of selected meteorological stations and the mean of the climate indices within a broader area. No study has been done in case of Sarawak, which employed the usage of the ETCCDI indices and gridded-based datasets which provide the opportunity for a finer resolution of spatio-temporal information for extreme climates. Therefore, the usage of Princeton gridded-based datasets with the longest and continuous spatio-temporal resolution was applied, to capture the long-term climatic trend over the climate sensitive peatland region of Sarawak. The study makes important contributions to the climate change research for the region and will add to the supplementary understanding of climate change impact on tropical peatland which is susceptible to climate change.

## 2. Study area and sources of data

The study area is situated in ~1.6 Mha of Sarawak peatland found principally along the low-lying alluvial coastal plain, extending over 750 km along the north-western coast as shown in Fig. 1. Geographically, Sarawak and its peatland is positioned in the centre of the Maritime Continent between latitude 0°50′N and 5°N and longitude 109°36′E and 115°40′E, closely north of the equator. The peat swamp forest of Sarawak generally has a yearlong high water table, and high soil moisture because the forest settings are highly humid, damp and heavily shaded with a closed canopy ecosystem (Kreitmeier et al., 2015; Ngau et al., 2022). The forest ground was covered with thick fibrous roots and undecomposed litter of leaf and branches. Sarawak peatland has been logged over the years and utilized for agricultural activities particularly for oil palm, sago and rubber where compaction and drainage is a precondition. Copious rainfall, high humidity and uniform temperature characterized the tropical equatorial climate of Sarawak (Tangang et al., 2013). The Köppen-Geiger climate classification characterized this region as Tropical Rainforest (*Af*), with annual rainfall ranging between 3 300 mm close to the coastland and 4 600 mm further inland (Kottek et al., 2006).

Out of 58 rainfall station initially being assessed in this study, 27 rainfall and 4 temperature stations with the longest and reliable temporal continuity and fairly distributed across Sarawak peatland were selected for validation of the gridded-based Princeton datasets. Rainfall and temperature stations data was retrieved from the Department of Irrigation and Drainage (DID) of Malaysia and Berkeley Earth (Berkeley Earth, 2018) respectively. The stations were chosen based on the availability of the continuous and homogeneous historical records for the period of 1960–2010 with less than 20% missing values in each year. However, different starting years for rainfall records were used due to the gap and inhomogeneity in the time series. This should be borne in mind when the validation results were discussed. The average temperature records were available for the period of 1960–2010. Station information including station number, basin, coordinates and the period of record, were given in Table 1.

To reveal long-term climate trends, at least 30 years of climate data are recommended for climate assessment (Mckee et al., 1993). This is because trends based on shorter time series are highly sensitive to values at the start and end of the series. Larger periods than 30 years are sufficiently independent in climatological time series when handled with inherent variability, as per World Meteorological Organization (WMO) guidelines (Arguez and Vose, 2011). The Princeton data sets provided by Terrestrial Hydrology Research Group from Princeton University and available at the website, http://hydrology.princeton.edu/data.pgf.php, was used in this study with a spatial resolution of 0.25°. Daily rainfall, TX and TN data sets with the longest period available at the beginning of this study, spanning 68-years from 1948 to 2016 at 47 grid points (Fig. 1) covering the whole peatland area of Sarawak were retrieved and used.

There are 27 core indices (the ETCCDI indices) of climate extreme available through RClimDex, recommended by Expert Team on Climate Change Detection, Monitoring and Indices (ETCCDMI) with primary focuses on extremes (Peterson et al., 2001; Zhang et al., 2005). 25 indices relevant to the tropical region of Sarawak including TA, TX and TN were applied in this study as listed in Table 2. These indices were selected because extreme rainfall and temperature are two main climate component governing the local natural climate in Sarawak and play an important role for agricultural production. Due to climate change, extreme rainfall and temperature are likely to occur in tropical regions of Southeast Asia more frequently which will enhance the already high

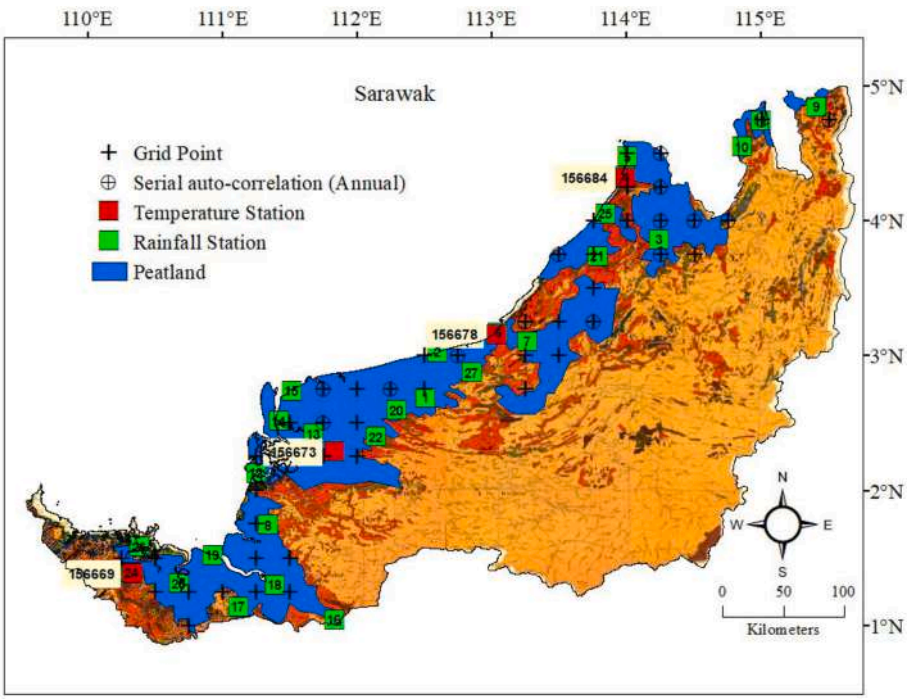


**Fig. 1.** Sarawak soil map with 27 rainfalls and 4 temperature stations (light yellow label = station no.) and 47 grid-based Princeton climate data covering the peatland area. Grid point (suncross symbol) indicate that there is significant auto-correlation in the annual time series. (For interpretation of the references to colour in this figure legend, the reader is referred to the Web version of this article.)

flood and drought risks, particularly across the climate-sensitive area of tropical peatland (Ge et al., 2019). As far as the authors' knowledge, no study has been done in Sarawak utilizing the ETCCDI indices to provides fundamental characteristics analysis of extreme climate. In addition, these indices are relevant in all part of the world, allowing comparison between different regions. (Yin and Sun, 2018).

## 3. Methods

### 3.1. Data quality control

A rigorous data quality assessment was done to ensure a reliability validation process of Princeton gridded-based dataset, and the subsequent climate extreme assessment. The imputation of missing data for 27 rainfall stations was done by using nearest neighbor method due to its conceptual simplicity (Ferrari and Ozaki, 2014) by using R-based program, RClimTool (Llanos-Herrera, 2014). As the low range of missing data (0–6.7%) was observed in the time series, the nearest neighbor method was applied by using auxiliary information from the neighboring rainfall stations to initially detect any observable outliers, trends and potential discontinuities and breaks in the time series. The missing data was then imputed directly to lessen the amount of missing data and subsequently obtaining a continuous data series for each rainfall station (Ferrari and Ozaki, 2014). Then, to facilitate data quality assessment, the integrated R package, Multi-Site Auto-Regressive Weather GENerator (RMAWGEN) which make use of Vector AutoRegressive models (VARs) estimation in RClimTool was applied to fill the remaining missing data (Cordano and Eccel, 2011).

The evaluation of the quality control of the time series was assessed afterwards by using RClimTool to identify and replace unverified records in the database (Ferrari and Ozaki, 2014). The double mass curve for the annual time series was constructed after imputation and quality control processes to detect if there is any breakpoint. Temperature datasets were excepted from the imputation process because it has been subjected to internal adjustment and data quality control by Berkeley Earth. Nonetheless, the presence of outliers were identified in daily rainfall, TX, and TN which was then checked with neighboring stations for consistency or potential breaks. The annual and monthly mean temperature (total for rainfall) series were then prepared and examined for discontinuities. A sufficiently long record of daily data which passed with these quality control and homogeneity procedures were subsequently used to validate and to assess the capability of the gridded-based Princeton datasets in simulating the local climate. Even though Princeton datasets has been validated and utilized in many part of the world, the validation under tropical climate is still low. Therefore, the validation process in this study will contribute to the reliability assessment of the Princeton datasets in tropical climate, in case of Sarawak.

### 3.2. Extreme climate data preparation and validation

The extreme climate for rainfall and temperature indices were computed by using R-based software package, RClimDex, developed at the Climate Research Branch of Meteorological Service of Canada on behalf of the ETCCDMI. RClimDex and its documentation can be found at http://etccdi.pacificclimate.org/software.shtml. In this study, 25 indices relevant to Sarawak's tropical climate, including TX and TN, were used, as shown in Table 2. An annual and seasonal time-series of each index was computed for each 47 grid point. Hence, the indices convey information about events with the most extreme magnitude annually and seasonally. The areal average of rainfall and temperature data were used for the validation of gridded-based Princeton datasets. Validation was also done by visualization of the time series, construction of scatter plot, probability distribution function (PDF), student's t-test and statistical performance indices, namely normalized root mean square error (NRMSE), percent bias (PBIAS), Nash–Sutcliffe efficiency (NSE), modified index of agreement (MD), coefficient of determination ($R^2$) and volumetric efficiency (VE). This widely used statistical performance was employed as it has been used by other studies in hydrology and climatology time series (Iqbal et al., 2021; Navidi Nassaj et al., 2022; Salehie et al., 2022; Tan et al., 2021).

**Table 1**
List and general information of 27 rainfall stations and 4 Temperature stations in Sarawak peatland used in this study.

| Rainfall Station Information | | | | | | |
|---|---|---|---|---|---|---|
| No | Station No. | Basin | Lat | Long | Period | NA* (%) |
| 1 | 2625051 | Balingian | 2.69 | 112.50 | 1989–2010 | 5.6 |
| 2 | 3025001 | Balingian | 3.03 | 112.59 | 1979–2010 | 6.3 |
| 3 | 3842034 | Baram | 3.86 | 114.24 | 1983–2010 | 2.1 |
| 4 | 4339005 | Baram | 4.33 | 113.99 | 1982–2010 | 0 |
| 5 | 4440001 | Baram | 4.48 | 114.00 | 1973–2010 | 0.2 |
| 6 | 3130002 | Kemena | 3.17 | 113.04 | 1973–2010 | 0 |
| 7 | 3132023 | Kemena | 3.11 | 113.26 | 1984–2010 | 4.5 |
| 8 | 1713005 | Krian | 1.74 | 111.33 | 1984–2010 | 0 |
| 9 | 4854009 | Lawas | 4.85 | 115.4 | 1989–2010 | 0 |
| 10 | 4548004 | Limbang | 4.55 | 114.85 | 1984–2010 | 5.4 |
| 11 | 4749001 | Limbang | 4.74 | 115.00 | 1984–2010 | 0 |
| 12 | 2115008 | Lower Rajang | 2.13 | 111.25 | 1986–2010 | 0 |
| 13 | 2412001 | Lower Rajang | 2.42 | 111.67 | 1986–2010 | 3.9 |
| 14 | 2514004 | Lower Rajang | 2.51 | 111.42 | 1998–2010 | 6.7 |
| 15 | 2712001 | Lower Rajang | 2.74 | 111.51 | 1984–2010 | 3.1 |
| 16 | 1018002 | Lupar | 1.04 | 111.83 | 1984–2010 | 1.2 |
| 17 | 1111008 | Lupar | 1.14 | 111.11 | 1977–2010 | 3.7 |
| 18 | 1313006 | Lupar | 1.30 | 111.39 | 1964–2010 | 3.7 |
| 19 | 1509009 | Lupar | 1.52 | 110.92 | 1984–2010 | 0.2 |
| 20 | 2522038 | Mukah | 2.60 | 112.29 | 1990–2010 | 0 |
| 21 | 3737045 | Niah | 3.74 | 113.78 | 1985–2010 | 5.6 |
| 22 | 2321001 | Oya | 2.40 | 112.13 | 1989–2010 | 3.3 |
| 23 | 1306055 | Sadong | 1.31 | 110.67 | 1966–2010 | 6 |
| 24 | 1303014 | Samarahan | 1.39 | 110.32 | 1982–2010 | 0.5 |
| 25 | 4038006 | Sibuti | 4.06 | 113.84 | 1982–2010 | 3.8 |
| 26 | 1503007 | Sungai Sarawak | 1.58 | 110.38 | 1977–2010 | 0 |
| 27 | 2828025 | Tatau | 2.88 | 112.85 | 1985–2010 | 0 |
| Temperature Station Information | | | | | | |
| No | Station No. | Basin | Lat | Long | Period | NA** (%) |
| 1 | 156, 669 | Sg. Sarawak | 1.38 | 110.33 | 1960–2010 | – |
| 2 | 156, 673 | Lower Rajang | 2.29 | 111.83 | 1960–2010 | – |
| 3 | 156, 678 | Kemena | 3.16 | 113.03 | 1960–2010 | – |
| 4 | 156, 684 | Miri | 4.32 | 113.99 | 1960–2010 | – |

NA* = Missing value observed after imputation by using the nearest neighboring method.
NA** = Temperature datasets has been subject to Berkeley Earth quality control procedures and adjustment.

### 3.3. Mann-Kendall and Modified Mann-Kendall test

To explore the trends in hydro-climatological time series, the World Meteorological Organization (WMO) has recommended non-parametric MK test (Peterson et al., 2001) and this approach was used in this work trend detection. As per, Koutsoyiannis and Montanari (2007), MK trend tests statistic is susceptible to the scaling behavior and this significantly increases the pattern of trends. Hence, numerous studies have doubted the previously obtained results due to the multi-decadal variability in time-series (Ehsanzadeh and Adamowski, 2010; Fathian et al., 2014; Lacombe et al., 2012; Shahid et al., 2014). The MK method was modified by Hamed (2009, 2008) to accommodate the scaling effect and this improved the power of the tests in discriminating multi-scale variability of unidirectional time series trends. Thus, the m-MK tests are also employed in the present study to confirm the significance of MK test at 95% significant level for 25 selected 'ETCCDI' (Table 2) across 47 homogeneous Princeton grid points of Sarawak peatland.

MK trend test calculation involved comparison of each data value with all following data values of the ordered data sample. Here, the time series $x_1$, $x_2$, $x_3$ …, and $x_n$ of the Mann Kendall statistic ($S$) is computed as,

$$S = \sum_{k=1}^{n-1} \sum_{i=k+1}^{n} \text{sign}\ (x_i - x_k)$$

**Table 2**
List of climate extreme indices used in this study (Frich et al., 2002; Karl et al., 1999; Peterson et al., 2001).

| Indicator name | Definitions | Units |
|---|---|---|
| TA | Average temperature | °C |
| TX | Maximum temperature | °C |
| TN | Minimum temperature | °C |
| Max TX (TXx) | Monthly maximum value of daily maximum temperature | °C |
| Max TN (TNx) | Monthly maximum value of daily minimum temperature | °C |
| Min TX (TXn) | Monthly minimum value of daily maximum temperature | °C |
| Min TN (TNn) | Monthly minimum value of daily minimum temperature | °C |
| Cool nights (TN10p) | Percentage of days when TN < 10th percentile | Days |
| Cool days (TX10p) | Percentage of days when TX < 10th percentile | Days |
| Warm nights (TN90p) | Percentage of days when TN > 90th percentile | Days |
| Warm days (TX90p) | Percentage of days when TX > 90th percentile | Days |
| Warm spell duration index (WSDI) | Annual count of days with at least 6 consecutive days when TX > 90th percentile | Days |
| Cold spell duration index (CSDI) | Annual count of days with at least 6 consecutive days when TN < 10th percentile | Days |
| DTR | Monthly mean difference between TX and TN | °C |
| Max 1 day precipitation amount (Rx1day) | Monthly maximum 1-day precipitation | mm |
| Max 5 day precipitation amount (Rx5day) | Monthly maximum consecutive 5-day precipitation | mm |
| Simple daily intensity index (SDII) | Annual total precipitation divided by the number of wet days (defined as rain ≥ 1.0 mm) in the year | mm/day |
| Number of heavy precipitation days (R10) | Annual count of days when rain ≥ 10 mm | Days |
| Number of very heavy precipitation days (R20) | Annual count of days when rain ≥ 20 mm | Days |
| Number of days above 27 mm (Rnn) | Annual count of days when rain ≥ nn mm, nn is user defined threshold | Days |
| Consecutive dry days (CDD) | Maximum number of consecutive days with RR < 1 mm. | Days |
| Consecutive wet days (CWD) | Maximum number of consecutive days with RR ≥ 1 mm | Days |
| Very wet days (R95p) | Annual total prcp when RR > 95th percentile | Days |
| Extremely wet days (R99p) | Annual total prcp when RR > 99th percentile | mm |
| Annual total wet-day precipitation (PRCPTOT) | Annual total prcp in wet days (RR ≥ 1 mm) | mm |
| Number of tropical nights (TR) | Annual count of days when TN (daily minimum temperature) > 20 °C. | mm |

where sign

$$(x_i - x_k) = \begin{cases} +1 \text{ if } (x_i - x_k) > 0 \\ 0 \text{ if } (x_i - x_k) = 0 \\ -1 \text{ if } (x_i - x_k) < 0 \end{cases} \quad (1)$$

To statistically quantify the trend significance employing normalized test statistic $Z$, the associated probability of $S$ and the sample size, $n$, is afterwards computed as follow,

$$Z = \begin{cases} \dfrac{S-1}{\sqrt{Var\ (S)}} \text{ if S} > 0 \\ 0 \quad \text{if S} = 0 \\ \dfrac{S+1}{\sqrt{Var\ (S)}} \text{ if S} < 0 \end{cases} \quad (2)$$

The computation for variance, Var*(S)* for the above normalized test

statistic $Z$, is as follow,

$$Var(S) = \frac{n(n-1)(2n+5) - \sum_{i=1}^{m} t_i(t_i-1)(2t_i+5)}{18} \quad (3)$$

where the data points number is denoted as $n$, the set with the same value of sample data of a tied number group denotes as $m$, and the number of the extended ties $i$, denotes as $t_i$. Based on the positive or negative value of the normalized test statistic $Z$, increasing or decreasing trends are indicated. Significance level of 95% was used in the study to determine the significant change. Here, if $|Z| > 1.96$; and at 95% significance level, the null hypothesis of no trend is rejected. If $|Z| > 1.645$; and at 95% significance level, the null hypothesis of no trend is rejected.

The de-trended series based on the ranking of the equivalent normal variants for the calculation of m-MK test were attained by using the following equation,

$$Z_i = \varphi^{-1}\left(\frac{R_i}{n+1}\right) for\ i = 1:n \quad (4)$$

where the de-trended series is denote as $R_i$, time series length denote as $n$, and the inverse standard normal distribution function, with mean value of 0, and standard deviation of 1, is denote as $\varphi^{-1}$.

The function of log likelihood in McLeod and Hipel (1978) was maximised to calculate the scaling coefficient or Hurst coefficient, $H$. When true $H$ is 0.5, this assessment of H is assumed to be normally distributed in the uncorrelated case. The following equation is used to calculate the correlation matrix for $H$,

$$C_n(H) = \left[\rho_{|j-i|}\right], for\ i = 1:n, j = 1:n \quad (5)$$

$$\rho_l = \frac{1}{2}\left(|l+1|^{2H} - 2|l|^{2H} + |l-1|^{2H}\right) \quad (6)$$

where, for a given $H$, $\rho_l$ is denoted as the autocorrelation function of lag $l$ which for the constructed time series is independent from aggregation (Koutsoyiannis and Montanari, 2007). Subsequently, the calculated $H$ can be obtained as follow,

$$\log L(H) = -\frac{1}{2}\log|C_n(H)| - \frac{Z^{\tau}[C_n(H)]^{-1}Z}{2\gamma_o} \quad (7)$$

Where the determinant of correlation matrix $[C_n(H)]$ is denote as $|C_n(H)|$, the transpose vector of equivalent normal variates $Z$, $[C_n(H)]^{-1}$ is denote as $Z^{\tau}$, the inverse matrix is $[C_n(H)]^{-1}$, and the variance of $z_i$ is denote as $\gamma_o$. The maximum $\log L(H)$ is determined as the value of $H$ for the time series $x_i$. The value of $H$ is solved in this study between 0.50 and 0.98 with an increasing step of 0.01. When $H = 0.5$ (normal distribution), the mean ($\mu_H$) and standard deviation ($\sigma_H$) can be used to computed the 5% significance level of $H$ by using the equation provided by (Hamed, 2009) as follow,

$$\mu_H = 0.5 - 2.87n^{-0.9067}$$

$$\sigma_n = 0.7765n^{-0.5} - 0.0062 \quad (8)$$

If $H$ is found to be statistically significant, the variance of $S$ is obtained for given $H$ as follow,

$$V(S)^{H'} = \sum_{i<j}\cdot\sum_{k<l}\frac{2}{\pi}\sin^{-1}\left(\frac{\rho|j-i| - \rho|i-l| - \rho|j-k| + \rho|i-k|}{\sqrt{(2-2\rho|i-j|)(2-2\rho|k-l|)}}\right) \quad (9)$$

Where $V(S)^{H'}$ is denote as the estimated bias by calculating $\rho_l$ for a given $H$ by using equation (6). On the other hand, the following equation (10) was used to calculate $V(S)^{H}$, unbiased estimate, by multiplication of the bias correcting factor $B$,

$$V(S)^{H} = V(S)^{H'} \times B \quad (10)$$

where, $B$ is a function of $H$ as shown below,

$$B = a_0 + a_1H + a_2H^2 + a_3H^3 + a_4H^4 \quad (11)$$

In equation (11), the sample size $n$ are based on the function of the coefficients, $a_0$, $a_1$, $a_2$, $a_3$, and $a_4$ (Hamed, 2008). As provided in the previous equation (2), $V(S)^{H}$ was replace with $V(S)$ to determine the significance of the MK test.

Kendall's tau based slope estimator was used to calculate the magnitude of the observed trend at 95% significance level (Sen, 1968). Because of its robustness against the effect of outliers in time series, this estimator has been broadly used in hydro-meteorological studies (Zhang et al., 2005). All of the paired data are calculated to derive an estimate of the slope $Q$ as follow,

$$Q_i = \frac{x_j - x_k}{j-k}, i = 1,2,\ldots N, j > k \quad (12)$$

$N = n(n\text{-}1)/2$ slope estimates $Q_i$ can be determine, if there are $n$ values $x_j$ in the time series. The median of the values of $N$ associated with $Q_i$, is the slope estimated by Sen's. These median of all slopes, are ranked from the lowest to the highest $Q_i$ based on the slopes value of $N$ as follow,

$$Q_{med} = \begin{cases} Q_{|(N+1)/2|} & if\ N\ is\ odd \\ \dfrac{Q_{|N/2|} + Q_{|(N+2)/2|}}{2} & if\ N\ is\ even \end{cases} \quad (13)$$

## 4. Application results

In Sarawak peatland, the highest annual rainfall was recorded in 2008 at 4 355 mm (not shown) coincide with strong La Niña event (Arndt et al., 2010) and the lowest annual rainfall was recorded in 1972 at 2 909 mm (not shown) coincide with strong El Niño event (Vose et al., 2014). High amount and high intensity rainfall, occurring throughout the months of November to March characterized the NE monsoon, while a relatively prolonged dry period characterized the SW monsoon during the months of May to September (Dindang et al., 2013; Diong et al., 2015). The NE and SW monsoon recorded annual mean of 1 697 mm and 1 243 mm respectively with the highest monthly rainfall on the month of January at 395 mm and the lowest monthly rainfall on the month of July at 208 mm. During the inter-monsoon months of April and October, high spatial variability of rainfall happens due to the locally driven convective activities (Joseph et al., 2008). Linear regression (not shown) showed that temperature is increasing for average temperature (TA), TX, and TN at annual rate of 0.0057 °C ranging between 25.8°C-27.2 °C, 0.0026 °C ranging between 30.0°C-31.7 °C and 0.0088 °C ranging between 21.5°C-23.3 °C respectively. Temperatures are increasing more at nights than during the days indicating an overall trend of decreasing DTR.

ENSO events play a key role in governing the seasonal extremity of NE and SW monsoon across Sarawak. El Niño and La Niña are the extreme phases of the ENSO cycle. During El Niño, there is a warming of the ocean surface in the central and eastern tropical Pacific Ocean. Over the maritime continent which consists of Malaysia, Indonesia, New Guinea and the surrounding land and oceanic areas (including Sarawak), the easterly wind weakens and rainfall tends to become reduced. Meanwhile, during La Niña there is a cooling of the ocean surface in the central and eastern tropical Pacific Ocean. On the contrary, there is a cooling of the ocean surface during La Niña causing the easterly wind to become stronger than normal along the equator and rainfall tends to increase across the maritime continent. It is widely known that during El Niño years, droughts tend to occur over the maritime continent (Gomyo and Kuraji, 2009). During the La Niña, heavy rainfall happens which usually leads to flooding.

In Niño-3.4 area (5°S–5°N, 170°–120°W) where Sarawak was located, Niño-3.4 sea surface temperature (SST) anomaly reached a maximum during the DJF (December, January, February) warm phase

(La Niña) and JJA (June, July, August) cool phase (El Niño) of the ENSO (Rasmusson and Carpenter, 1982). Both of these ENSO events coincide with the NE and SW monsoon, respectively. It was found by Gomyo and Kuraji (2009) that ENSO-rainfall relationship during JJA give a stronger negative correlation in the Southwest of Sarawak whereas during DJF, a stronger negative correlation shifted northeastward of Sarawak. Therefore, as the ENSO event becomes more extreme due to climate change, the NE and SW monsoon which affect the local climate in Sarawak is expected to become more extreme as well as it coincides with the maximum anomaly of the ENSO event. Juneng and Tangang (2005) suggested that the possible mechanism of such correlation can be associated with the anomalous cyclonic/anticyclonic circulation that stipulated to be a downstream response to the boomerang-shaped SST anomalies. These confirm the influence of decadal-scale climatic factors (ENSO) affecting the local climate which increase the extremity of high rainfall event during the NE monsoon (coincide with La Niña) and drier period during the SW monsoon (coincide with El Niño).

An estimate of the auto-correlation function of a time series for annual (18 out of 47 grid point) as shown in Fig. 1, and monthly (all 47 grid point) rainfall showed that there is significant positive serial autocorrelation which signify the influence of natural climate variability in the study area (Hyndman, 2015). Significant positive serial auto-correlation was also found for all grid points for annual and monthly TA time series. The results indicate a constant rate of increase in spatial and temporal autocorrelation over time for monthly rainfall, and for both annual and monthly TA across Sarawak tropical peatland due to climate change, which is similar in other studies (Barnston et al., 2020; Di Cecco and Gouhier, 2018; Liu et al., 2019; Rousta et al., 2017). This could be caused by the substantial influence of regional climate upon exposure to different atmospheric conditions, as well as in-situ synoptic systems, such as Madden Julian Oscillation (MJO), ENSO, Indian Ocean Dipole (IOD), Asian-Australian monsoon, and the localized land-sea breezes. There has been increases in ENSO-induced changes of the South China Sea which, during El Niño, increased the westward Luzon Strait through flow, thereby forcing a warmer surface water to flow into the northern Makassar Strait and subsequently pass through the north-western coast of Sarawak (Gordon et al., 2012). Consequently, the northern coastal peatland of Sarawak would be subject to higher natural climate variability than other regions which has been further confirmed by Gomyo and Kuraji (2009). Another recent study by Che Ros et al. (2016) also confirms that ENSO plays a key role that causes sudden increase in variability of long-term rainfall in Kelantan River basin. Break points in temperature time series also have been found by Suhaila and Yusop (2018) which possibly related to climatic factors, such as El Niño and La Niña events. Therefore, in addition to MK, there is a need to employ m-MK which is capable of distinguishing unidirectional trend with multi-scale variability due to the influence of climate variability.

### 4.1. Rainfall data quality

It has been observed that the selected rainfall stations in Sarawak were subject to missing values of less than 20%, discontinuities and different starting and end dates. Table 1 presents the rainfall records with missing values less than 6.7% after imputation through the nearest neighbor method. All the missing values were then filled afterwards by using RClimTool. A quality control (QC) log file was created for every station to document each change or acceptance of an outlier. The information derive from the QC log file were percentage of data within and outside the predefine limits and range of mean and standard deviation, identifying the cases of TX lower than TN, percentage of days of temperature variation higher or equal than 10 °C, identifying equal data in a period of longer than five consecutive days and the presence of outliers. A preliminary report consists of graphical and descriptive analysis (Plot Charts, Graphs, Scatter plots or Boxplot) made by the application was also being assessed (result not shown). The double mass curve for the annual and monthly rainfall showed no breakpoint in the time series (not shown) which indicates good consistency of the rainfall data after imputation. The sequential student's t-test was then applied to the different subsets of the time series data at each station for homogeneity evaluation by determining whether or not a potential shifting point exists between the imputed rainfall station and gridded-based Princeton time series. The acquired *t*-test statistics for all stations were found between 0.71 and 0.90. As the critical t-values were much higher compared to the test statistics at 0.05 significance level, it can be concluded that potential discontinuity does not exist in the time series at any station after imputation. As a number of statistical, graphical, and descriptive analysis has been done for the imputed rainfall station datasets, the subsequent analysis can be done to validate gridded-based Princeton datasets.

### 4.2. Validation of gridded-based data

The time series, scatter plot and PDF of both station and gridded-based Princeton datasets of rainfall and temperature was compared to show the efficacy of the Princeton datasets in capturing and simulating the local climate (Fig. 2). The detail on the statistical performance evaluation is presented in Table 3. The time series showed a high correlation of 0.84 (rainfall) and 0.83 (temperature). The shape of the PDF does not vary, showing a high associative probability between the datasets, with slightly higher kurtosis of Princeton rainfall data and slightly lower kurtosis of Princeton temperature data. In addition, the performance of the statistical analysis based on the various methods (Section 3.2) has been taken into consideration that the plots show a considerably good match. The $R^2$ and MD values were found at 0.71 and 0.72 respectively for rainfall, while 0.69 and 0.72 respectively for temperature which indicate there is less error variance. The NSE value for rainfall and temperature is 0.70 and 0.68 respectively while VE was found at 0.83 and 0.99. PBIAS was 5.1 and −0.1 for rainfall and temperature respectively and NRMSE was 55.1 for rainfall and 56.3 for temperature. Negative PBIAS was observed for temperature indicates only a slight overestimation of the extreme temperature event. The low errors and biases and near to 1 values of NSE, MD, $R^2$ and VE suggest the promising capability of Princeton data sets in replicating the daily rainfall and temperature of Sarawak peatland. Some inherent differences between datasets are to be expected because the datasets vary in their representation of coastal areas. Keeping in mind that the station's data was spatially less homogeneous than gridded-based datasets and has low representation along the coastline has caused the inherent differences between the datasets. In addition, high climate heterogeneity in rainfall and temperature was also observed in both space and time for station data.

### 4.3. Spatiotemporal distribution of seasonal trend

The results for the annual, regional average and monsoonal (NE and SW monsoons) trend of extreme climate in Sarawak peatland based on MK and m-MK at 95% significance level are shown in Table 4. The annual trend was assessed to revealed the annual changes of the extreme climate in relation with the annual and inter-annual influence of the climate phenomena. In addition, to get a general and broader view of trends across Sarawak peatland, the regional average trend was calculated based on the mean of 47 grid points for each extreme climate index. As monsoon play a major role in regulating the regional climate in a year over Sarawak, the changes in trend for both monsoon was also assessed. The table showed the number of grid points for each climate extreme indices that showed either significant increasing/decreasing (±) across Sarawak tropical peatland were detected under MK and m-MK trend test.

No significant change was detected by using m-MK test for regional trend, and a lower number of significant changes for annual and monsoonal trend was observed under m-MK test compared to MK test as

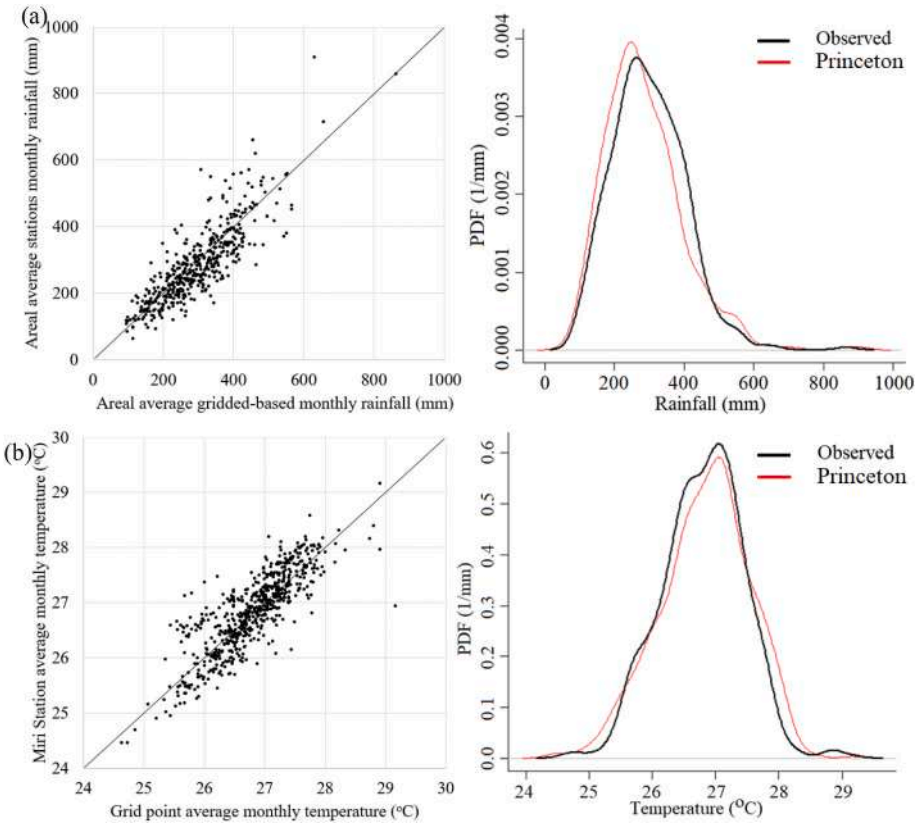


**Fig. 2.** Scatter plot and PDF of (a) monthly areal average of rainfall vs gridded-based Princeton dataset and (b) Miri temperature station with the nearest corresponding Princeton grid point for the period of 1973–2010 (rainfall) and 1960–2010 (TA) in Sarawak peatland. The selected Princeton grid points are based on Fig. 1.

**Table 3**
Statistical performance results for the validation of the monthly areal average of rainfall vs gridded-based Princeton dataset and Miri temperature station with the nearest corresponding Princeton grid point for the period of 1973–2010 (rainfall) and 1960–2010 (TA) in Sarawak peatland.

| | $R^2$ | MD | NSE | VE | PBIAS |
|---|---|---|---|---|---|
| Rainfall | 0.71 | 0.72 | 0.7 | 0.83 | 5.1 |
| Temperature (Miri Station) | 0.69 | 0.72 | 0.68 | 0.99 | −0.1 |

shown in Table 2. For the annual trend, both a significant increasing and decreasing trend was observed for extreme rainfall and temperature for 23 indices (MK) and 13 indices (m-MK). However, a significant reduction of the number of indices with significant trend was found under the m-MK test. Under m-MK test, there are only 11 indices with increasing trend (CDD, CSDI, CWD, R10, R20, Rnn, TN90p, TNn, TNx, WSDI and TR) and 7 indices with decreasing trend (CSDI, DTR, R10, Rnn, TN10p, WSDI and TR). Meanwhile, CSDI, R10, Rnn, WSDI and TR were showing both increasing and decreasing trends.

This is due to the capability of the m-MK test in removing the effect of serial auto-correlation due to the influence of high climate variability found in the time series. Ahmed et al. (2022) also found lower significant changes in long-term rainfall over India, observed under m-MK test compared to MK test. Another study by Rana et al. (2022) also showed no significant trend under m-MK test at the Chamoli and Pithoragarh district rainfall station in Uttarakhand, India that showed autocorrelation in annual rainfall and rainy days. These stations otherwise showed significant changes under the MK test. Longobardi and Boulariah (2022) also found a large difference in significant trend between MK and m-MK test with 80% and 73% respectively in inter-annual variability of precipitation in the Campania Region, Southern Italy. They also conclude that the m-MK test identifies a reduced number of stations displaying a significant trend, highlighting the potential effect of autocorrelation in the data that the MK does not account for. Therefore, for spatial analysis in this study, extreme climate results based on m-MK test which can discriminate the serial auto-correlation in the time series were further discussed between the NE and SW monsoon to evaluate the real impact of climate change.

In general, the NE (November to March) and SW (May and September) monsoons have a significant seasonal effect on the development of weather patterns in Borneo, shaping local and regional atmospheric convection (Sa'adi et al., 2021). For seasonal trends, 18 and 22 indices were significant under MK test for both NE and SW monsoon, respectively. However, a lower number of indices and grid points showing significant changes under m-MK test compared to MK test, emphasized that without removing the effect of serial auto-correlation, there will be exaggeration of changes in climatic trend. Hence, the spatial mapping of the extreme climate indices which only reveal significant trends under m-MK test will be discussed and are shown in Fig. 3 (NE monsoon) and Fig. 4 (SW monsoon).

DTR showed a higher distribution of significant decreasing trend during the NE monsoon (7 grid) compared to SW monsoon (5 grid) at the central-coastal region as temperature at night warms more than during the day. The results were concurrent with a significantly increasing trend of extreme minimum temperature indices of TNn and TN90p in these regions. This suggests that the DTR is decreasing in the central-coastal region during the NE monsoon. Other studies also found a decreasing DTR due to climate change. For example, Qu et al. (2014) found a steady decrease of annual DTR in the United States over the past decades. Based on the newly developed China Meteorological Administration–Land Surface Air Temperature (CMA-LSAT) dataset employed by Sun et al. (2019), there is a large significant decrease in global land DTR from 1951 to 2014. In Sarawak, there is an inverse relationship between DTR and monsoon rainfall throughout the year. As extreme

**Table 4**
Trend results for extreme climate in Sarawak peatland. Significant increasing and decreasing trends was represented by (+) and (−), respectively.

| No | Indices | Annual | | Regional average | | NE | | SW | |
|---|---|---|---|---|---|---|---|---|---|
| | | MK | m-MK | MK | m-MK | MK | m-MK | MK | m-MK |
| 1 | CDD | | 5(+) | | | | | | |
| 2 | CSDI | 9(+), 1(−) | 5(+), 5(−) | | | | | | |
| 3 | CWD | | 8(+) | | | | | | |
| 4 | DTR | 27(−) | 2(−) | – | | 26(−) | 7(−) | 26(−) | 5(−) |
| 5 | PRCPTOT | 2(+) | | | | 13(+) | | 3(−) | |
| 6 | R10 | 25(+), 3(−) | 15(+), 1(−) | + | | 31(+), 1(−) | 14(+), 1(−) | 4(+) | 17(+), 1(−) |
| 7 | R20 | 17(+), 1(−) | 21(+) | | | | 17(+) | 29(+) | 30(+), 3(−) |
| 8 | Rnn | 18(+), 1(−) | 21(+), 1(−) | | | 1(+) | 10(+) | 32(+), 3(−) | 22(+), 2(−) |
| 9 | R95p | 13(−) | | | | 2(−) | | 3(−) | 1(−) |
| 10 | R99p | 12(−) | | | | | | 1(−) | |
| 11 | Rx1day | 8(−) | | – | | 23(−) | | 30(−) | |
| 12 | Rx5day | 3(−) | | | | | | 17(−) | |
| 13 | SDII | 6(−) | | | | | | 19(−) | 1(−) |
| 14 | TA | 46(+) | | + | | 43(+) | | 47(+) | |
| 15 | TX | 27(+) | | | | 7(+) | | 29(+) | |
| 16 | TN | 47(+) | | + | | 44(+) | | 46(+) | |
| 17 | TN10p | 26(−) | 1(−) | – | | 37(−) | | 40(−) | |
| 18 | TN90p | 21(+), 2(−) | 11(+) | + | | 46(+) | | 47(+) | 3(+) |
| 19 | TNn | 14(+) | 6(+) | | | 30(+) | 10(+) | 36(+) | |
| 20 | TNx | 47(+) | 16(+) | + | | 47(+) | | 47(+) | |
| 21 | TX10p | | | | | 4(−) | | 29(−) | |
| 22 | TX90p | 1(−) | | | | 2(+) | | 23(+) | |
| 23 | TXn | 15(+) | | + | | 6(+) | | 34(+) | 1(+) |
| 24 | TXx | 16(+) | | | | 21(+) | | 8(+) | |
| 25 | WSDI | 1(+), 1(−) | 6(+), 6(−) | | | | | | |
| 26 | TR | 18(+), 4(−) | 12(+), 1(−) | + | | 44(+) | | 47(+) | |

MK = Mann-Kendall test; m-MK = modified Mann-Kendall test; NE = Northeast monsoon; SW = Southwest monsoon.

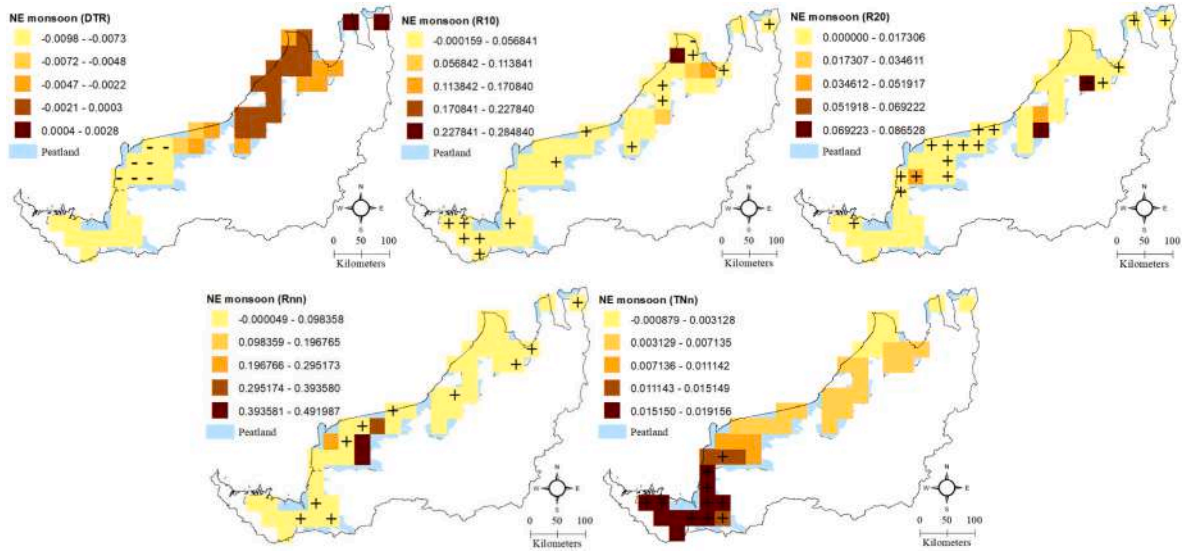


**Fig. 3.** NE monsoon trend for DTR, R10, R20, Rnn and TNn for the period of 1948–2016 under m-MK test at 95% significance level. Increasing and decreasing trends were represented by (+) and (−), respectively.

climates have been altered due to climate change, the regional climatological features including DTR are decreasing more, forming a stronger inverse relationship with rainfall (Beule and Tantanee, 2014; Kim and Bae, 2021). The stronger inverse relationship might be due to increased evaporation at night as temperature rises, producing more cloudy nights and rainfall (Qu et al., 2014). Decreasing DTR is becoming a concern for wildlife conservation as it may cause some climate-sensitive animals and plants to shift their distribution and even loss of population due to the changing physiological limits (Scheffers et al., 2014).

Low intensity rainfall (R10) was found to significantly increase at the south and northern region for NE (14 grid) and SW (17 grid) monsoon, although more homogeneous and regionally localized distribution was found during SW monsoon. This indicates that due to climate change, low rainfall distribution has become more sporadic and distributed over the years across tropical peatland of Sarawak. However, there is a difference in terms of high intensity rainfall (R20 and Rnn) spatial distribution between the NE and SW monsoon. High intensity rainfall (R20) showed higher distribution of significant increasing trend during the SW monsoon (30 grid) than NE monsoon (17 grid). The significant changes were found across all regions during SW monsoon, while changes were found to be concentrated at the central-coastal region during NE monsoon. The results indicate that a relatively drier period of SW monsoon will received rain in the form of higher intensity rainfall across the tropical peatland of Sarawak, providing a relief for water availability, storage, and recharge for natural ecosystem and agricultural

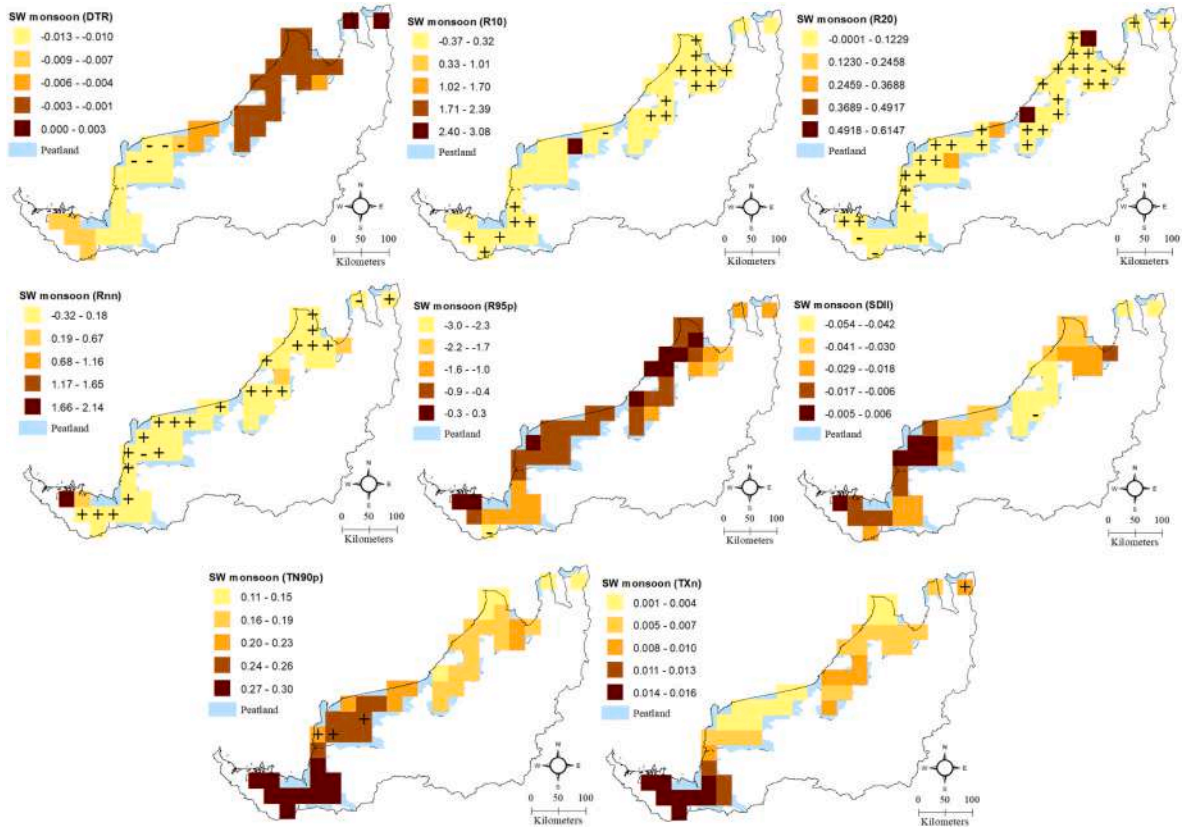


**Fig. 4.** SW monsoon trend for DTR, R10, R20, Rnn, R95p, SDII, TN90p and TXn for the period of 1948–2016 under m-MK test at 95% significance level. Increasing and decreasing trends were represented by (+) and (−), respectively.

activity. However, a high intensity rainfall at the central-coastal region during NE monsoon might worsen the flood condition that has been frequently recorded in the area (Asmat et al., 2021; Yiiong and Bundan, 2018). Similarly, very high intensity rainfall (Rnn) was found to be more significantly increased and widespread across Sarawak peatland during the SW monsoon (22) than NE monsoon (10). Increases in high rainfall intensity were found to be similar within other regions in Malaysia. For example, Mayowa et al. (2015) showed a significant increase in annual rainfall as well as rainfall during the monsoon on Peninsular Malaysia's east coast.

The monthly minimum value of minimum temperature (TNn) was found to significantly increase at the south (10 grid) during NE monsoon which might explain the increasing intensity of rainfall due to increased rate of evapotranspiration forming a cloudy night leading to rainfall event. Rainfall projection by Hussain et al. (2017) also suggested an increased rainfall over the southern and central-coastal region of Sarawak. Another study by (Hussain et al. (2015) also found an increasing projected rainfall over the northern region of Sarawak by using Statistical Downscaling Model (SDSM). Increase rainfall in these area during the NE monsoon might be due to increase influence of the ENSO-related rainfall anomalies associated to the seasonal modulation of the boreal summer intraseasonal oscillation, MJO activity and Borneo vortex genesis (Gomyo and Kuraji, 2009; Kurita et al., 2018).

On the contrary, a significant decreasing trend (1 grid) of percentile-based indices (R95p) was found during the SW monsoon as drier seasons become more extreme in the south. A stronger decreasing pattern of rainfall during the SW monsoon might explain the finding by Hin et al. (2009) which found a decreasing pattern of annual rainfall in Sarawak river located in southern Sarawak. Another study by Chiew et al. (2013) also found a decreasing trend of peak discharge in Sarawak river, indicating a decreasing rainfall pattern in the south of Sarawak. Rainfall intensity (SDII) was also found to significantly decrease at the central-coastal region (1 grid) during the SW monsoon. The distinct difference between increased rainfall during the NE monsoon and decreasing rainfall during the SW monsoon based on certain extreme climate indices in this study showed the importance of the monsoon in modulating the local climate. This difference would otherwise cannot be revealed based on the annual temporal pattern alone.

The upper end of percentile-based minimum temperature (TN90p) showed a significant increasing trend (3 grid) in the central-coastal region which might explain the increased intensity of rainfall (R20 and Rnn) in these regions due to increasing rate of evapotranspiration at night. Night-time warming may significantly decrease the oil palm and agricultural production in the central-coastal region of Sarawak tropical peatland (Zhang et al., 2021). However, increased intensity of rainfall (R20 and Rnn) may offset the negative effect of night-time warming. Meanwhile, the monthly minimum value of maximum temperature (TXn) was found to significantly increase (1 grid) in the north which might similarly cause higher rainfall intensity (R20 and Rnn) in these regions but during the day-time. Most of the extreme temperature indices have been found to increase across the world. A study by De Longueville et al. (2016) also found an increasing TN90P in Burkina Faso, showing night-time temperature is increasing more than day-time temperature. Another study by Sheikh et al. (2015) also found a significant increasing trend of TXn in Nepal and Pakistan. However, there is a mixed finding on the relationship between increased temperature and rainfall across the world with some regions showing increased rainfall and decreasing rainfall over another region (Sheikh et al., 2015). As there is a different large scale climate influence affecting the coastal-central region and the northern region of Sarawak, the increasing rainfall pattern during the relatively drier SW monsoon in the central-coastal and northern region of Sarawak might be due to the ENSO-related rainfall anomalies associated to the seasonal modulation of the boreal summer intraseasonal oscillation and MJO activity and

Borneo vortex genesis (Gomyo and Kuraji, 2009; Kurita et al., 2018). Overall, although rainfall intensity (SDII) was found to be decrease (significant at one grid point during the SW monsoon) across Sarawak peatland, certain indices of extreme rainfall showed that rainfall intensity (R10, R20, Rnn) has significantly increases either at night or day, due to significant changes of TX and TN.

The results for the seasonal trend were distinct from the annual trend which emphasized the importance of the monsoon in modulating the climate over Sarawak. It showed that the homogeneous climate pattern which characterized each of the monsoon with higher rainfall (NE monsoon) and drier period (SW monsoon) need to be evaluated separately to reveal the trend. Therefore, a clear picture of the climate over the region can only be properly derived based on the monsoon to understand the changes of the intensity and duration of the extreme climate over the region. The result also showed high spatial variability in terms of geographical distribution of significant trend depended on the indices.

## 5. Discussion

Present study showed that changes of extreme climate under the influence of climate change being detected under m-MK test have a lower number of significant changes compared to the MK test. It was expected that the high number of significant changes that was detected by employing MK test might be due to the effect of high climate variability in the time series. By removing the persistence of serial autocorrelation in the time series due to climate variability, m-MK test can be used to comparatively confirm the significant changes being detected by MK test.

The results suggest that significant changes in rainfall due to significant increase in temperature either at night and/or day will play a major role in modulating the extremity of the changing climate in Sarawak peatland. Higher rainfall intensity during the NE monsoon indicates that Sarawak peatland will be at risk of flood and inundation for a longer period than usual as peatland becomes saturated. This might affect the productivity of the agricultural land in the area. On the other hand, higher rainfall intensity during the SW monsoon does not mean that there will be more water available during the drier season. This is due to the amount of rain that falls intensely within a shorter period might not be able to compensate for higher temperature changes throughout the season, which may nevertheless, increase the fire risk. However, depending on the structural capability and management practice, it also can be argued that significant changes of extreme rainfall (R10, R20 and Rnn) being observed during the SW monsoon may have a profound effect on forest growth and agricultural productivity. Feher et al. (2017) reported that a slight change in extreme rainfall is expected to trigger relatively large changes in canopy growth. The availability of water through rainfall would help enhance rooting activity and growth of the plants, thus increasing productivity (Silins and Rothwell, 1998). Peat accumulation will also increase due to the inundation caused by higher water table and subsequently lower soil respiration in the area is expected as peat moisture content increases (van Huissteden et al., 2006).

Rainfall characteristics and trends may become more significant in the near future in conjunction with the increasing temperature as the optimum evaporation can be translated into rainfall. Increased air moisture may change rainfall behaviors in different ways, such as changes in daily intensity, seasonal distribution and inter-annual variability (IPCC, 2014). However, more investigation will be needed to project the future extreme climate pattern affecting the region. The increase in the number of hot days and warm nights, and the decrease in number of cool days and cool nights were observed in Sarawak peatland which is similar with a number of previous studies (IPCC, 2014; Manton et al., 2001; Tangang et al., 2006). The extremity of TN which increases more than TX, signifies an overall decreasing trend of DTR particularly in the central-coastal region. The results are similar as reported by Donat et al. (2013) that presented both daily TX and daily TN have turned out to be higher over the past years, but at different degrees: greater for TN than for TX values. Crop yield in peatland is expected to decline due to increased night time temperature because respiration losses as crop photosynthesis were sensitive to temperature changes (Peng et al., 2004).

It was also found that there is high spatio-temporal variability on how the extreme climate has changed across various regions in Sarawak. For example, under m-MK test, although most of the grid points showed a significant increasing trend for R10, R20 and Rnn during the SW monsoon, there is also a significant decreasing trend being detected. This spatial heterogeneity on the regional scale might be due to complex topography, land cover and irregular land masses across the island. Besides, there are various other climatic events such as Borneo Vortex, MJO, IOD and Asian-Australian Monsoon which affect various regions of Sarawak differently. The timing and intensity of these events over Sarawak may vary from region to region. Such that Borneo Vortex occurrence has a bigger impact in the Southwest region of Sarawak, while ENSO has a bigger impact in the Northwest region. Besides, complex topography and land cover might also play a key role in determining the local climate. Harrison (2005) reported that 1997–98 El Niño-induced severe droughts were reported in southern Borneo in September 1997 but they occurred in early 1998 in northern and eastern Borneo. However, due to station data limitation, no comprehensive study has been done to confirm the extent of the regional climate variability across Borneo and Sarawak in particular. Our results showed that within a finer regional scale, high spatio-temporal climate variability may persist. Therefore, further study will be needed to assess and confirm whether complex topography, land cover and certain climate events may influence the local climate.

The extreme rainfall and temperature trend in Sarawak peatland has changed and is expected to magnify in the coming decades. It is inferred that certain area of the peatland region will become drier due to increased evaporation and water loss cause by significant increasing trend of hot days (northern Sarawak) and warm nights (central-coastal region). Thus, it is crucial to devise a plan for water retention that can cater for extreme rainfall that falls within a shorter period in these area. Nonetheless, further works need to be done to clarify how the change in temperature might drive spatio-temporal changes in evaporation and water loss in a highly variable tropical climate. Increasing rates of soil respiration and decomposition will happen as the water table becomes lower with the increased intensity and frequency of the extreme temperature especially during the dry period. A more distinct seasonal pattern in the depth of the water table is expected as SW monsoon becomes drier than NE monsoon. Increasing temperature also means increasing decomposition rates of soil organic matter which subsequently increase the carbon release into the atmosphere. Increasing rate of respiration influenced by increasing extreme temperature is expected to occur in the peatland ecosystem which has denser decomposing litter layers. Peat moisture content is expected to decrease which can be correlated with an increase in peat decomposition as microbial activity increases (Davidson et al., 1998). Relative humidity would decline as extreme temperature increases significantly which would result in the higher rates of soil respiration. Thus, a decline in humidity would reduce the photosynthetic rate and plant productivity by depressing the response of stomatal opening to $CO_2$ (Talbott et al., 2003). In the coming years, the significant increasing trends of the extreme rainfall and temperature might magnify its role in determining soil temperature and soil respiration rates regardless of the type of ecosystem (van Huissteden et al., 2006).

It is expected that the peatland area which receives more rainfall will have a higher water table and the rate of decomposition will be inhibited as the production of peat will exceed its decay causing peat to accumulate (Cobb et al., 2017). On the contrary, peatland areas that receive less rainfall and are subject to high temperature will have lower water table whereas aerobic decomposition will increase and release carbon

(Cobb et al., 2017). By understanding the climatic trend over the peatland, we can devise a better water control system by conserving the water at the area prone to prolonged dry periods and systematically releasing the water at the area that receives intense rainfall.

## 6. Conclusion

The extreme climate trend based on the ETCCDI indices have been examined for extreme rainfall and temperature at 47 spatially homogeneous grid points in Sarawak peatland for the long-term historical period of 68-years from 1948 to 2016. The high spatio-temporal resolution of gridded-based Princeton climate data that was used to derive the extreme climate indices and trend in this study have not been used before in Borneo, particularly in Sarawak. The Princeton climate data provide homogeneously detailed analysis of extreme climate information across the region compared to station data and give higher confidence in the veracity of the reported trend. The application of RClimtool in choosing and testing of station data has facilitated the performance of quality control, filling missing data, homogeneity analysis and statistical analysis for the daily time series of rainfall and temperature. On the other hand, RClimDex offers a friendly graphical user interface to compute all selected 25 core climate change indices defined by ETCCDI.

The results obtained for the trend of extreme climate give evidence that global warming is not always observed everywhere spatially or temporally, because contrasting trends linked to specific local features can be deduced. Nevertheless, the trends observed under m-MK test which confirm the significant changes under MK test could have potential impacts on several biological and environmental sectors, in particular on biodiversity, forestry and agriculture. Extension of this approach to other parts of the world and ecosystem, where little is currently known regarding trends in extremes, would be valuable. Further study should be made to investigate and confirm the possible causes of the observed trends in extremes. The study is limited in terms of employing rainfall and temperature as the main input for extreme climate assessment. Therefore, other bioclimatic and environmental indices employing more input parameters that can assess climate impact on the environment and species range can also be explored (Amiri et al., 2020; Noce et al., 2020). The study can be extended to other tropical peatland regions in Southeast Asia to improve the understanding and relationship between the impact of climate extreme on this particularly sensitive ecosystem. In addition, there is also a number of gridded-based datasets with a good selection of climate parameters that can be employed for comparison with the current study such as ERA, APHRODITE, MERRA, TRMM, UDel, and GPCC among others, to improve the spatiotemporal resolution of the output. The relationship between GHG emission such as carbon dioxide, methane, and Nitrous oxide with the change in extreme climate affecting the tropical peatland due to climate change will be important for future carbon accounting in the region. Higher confidence in the certainty of future projection for extreme climate also could be subsequently pursued in future works.

## Authors statement

Zulfaqar Sa'adi: Data curation; Formal analysis; Methodology; Investigation; Visualization; Writing - original draft, - review & editing draft preparation; Resources; Software. Zaher Mundher Yaseen: Supervision, Conceptualization; Project administration; Writing - review & editing.

Aitazaz Ahsan Farooque: Formal analysis; Investigation; Visualization; Writing - original draft, - review & editing draft preparation.

Nur Athirah Mohamad: Formal analysis; Investigation; Visualization; Writing - original draft, - review & editing draft preparation. Mohd Khairul Idlan Muhammad: Formal analysis; Investigation; Visualization; Writing - original draft, - review & editing draft preparation. Zafar Iqbal: Formal analysis; Investigation; Visualization; Writing - original draft, - review & editing draft preparation.

## Declaration of competing interest

The authors declare that they have no known competing financial interests or personal relationships that could have appeared to influence the work reported in this paper.

## Data availability

Data will be made available on request.

## References


Adeyeri, O.E., Laux, P., Ishola, K.A., Zhou, W., Balogun, I.A., Adeyewa, Z.D., Kunstmann, H., 2022. Homogenising meteorological variables: impact on trends and associated climate indices. J. Hydrol. 607, 127585 https://doi.org/10.1016/J.JHYDROL.2022.127585.

Agnihotri, I., Punia, M.P., Sharma, J.R., 2018. Assessment of spatial variations in temperature and precipitation extremes in west-flowing river basin of kutch, Saurashtra and marwar, India. Curr. Sci. 114, 322. https://doi.org/10.18520/cs/v114/i02/322-328.

Ahmed, I.A., Salam, R., Naikoo, M.W., Rahman, A., Praveen, B., Hoai, P.N., Pham, Q.B., Anh, D.T., Tri, D.Q., Elkhrachy, I., 2022. Evaluating the variability in long-term rainfall over India with advanced statistical techniques. Acta Geophys. 801–818. https://doi.org/10.1007/S11600-022-00735-5, 2022 702 70.

Alamgir, M., Khan, N., Shahid, S., Yaseen, Z.M., Dewan, A., Hassan, Q., Rasheed, B., 2020. Evaluating severity–area–frequency (SAF) of seasonal droughts in Bangladesh under climate change scenarios. Stoch. Environ. Res. Risk Assess. https://doi.org/10.1007/s00477-020-01768-2.

Amiri, M., Tarkesh, M., Jafari, R., Jetschke, G., 2020. Bioclimatic variables from precipitation and temperature records vs. remote sensing-based bioclimatic variables: which side can perform better in species distribution modeling? Ecol. Inf. 57, 101060 https://doi.org/10.1016/J.ECOINF.2020.101060.

Ang, R., Kinouchi, T., Zhao, W., 2022. Evaluation of daily gridded meteorological datasets for hydrological modeling in data-sparse basins of the largest lake in Southeast Asia. J. Hydrol. Reg. Stud. 42, 101135 https://doi.org/10.1016/J.EJRH.2022.101135.

Arguez, A., Vose, R.S., 2011. The definition of the standard WMO climate normal: the key to deriving alternative climate normals. Bull. Am. Meteorol. Soc. https://doi.org/10.1175/2010BAMS2955.1.

Armal, S., Devineni, N., Khanbilvardi, R., 2018. Trends in extreme rainfall frequency in the contiguous United States: attribution to climate change and climate variability modes. J. Clim. 31, 369–385. https://doi.org/10.1175/JCLI-D-17-0106.1.

Arndt, D.S., Baringer, M.O., Johnson, M.R., 2010. State of the climate in 2009. Bull. Am. Meteorol. Soc. 91, s1–s222. https://doi.org/10.1175/bams-91-7-stateoftheclimate.

Asfaw, A., Simane, B., Hassen, A., Bantider, A., 2018. Variability and time series trend analysis of rainfall and temperature in northcentral Ethiopia: a case study in Woleka sub-basin. Weather Clim. Extrem. 19, 29–41. https://doi.org/10.1016/j.wace.2017.12.002.

Asmat, A., Wahid, S.N.S., Deni, S.M., 2021. Identifying rainfall patterns using Fourier series: a case of daily rainfall data in Sarawak, Malaysia. J. Phys. Conf. Ser., 12086 https://doi.org/10.1088/1742-6596/1988/1/012086, 1988.

Ayoub, A.B., Tangang, F., Juneng, L., Tan, M.L., Chung, J.X., 2020. Evaluation of gridded precipitation datasets in Malaysia. Rem. Sens. 12, 613. https://doi.org/10.3390/rs12040613.

Barnston, A.G., Lyon, B., Coffel, E.D., Horton, R.M., 2020. Daily autocorrelation and mean temperature/moisture rise as determining factors for future heat-wave patterns in the United States. J. Appl. Meteorol. Climatol. 59, 1735–1754. https://doi.org/10.1175/JAMC-D-19-0291.1.

Behnke, R., Vavrus, S., Allstadt, A., Albright, T., Thogmartin, W.E., Radeloff, V.C., 2016. Evaluation of downscaled, gridded climate data for the conterminous United States. Ecol. Appl. 26, 1338–1351. https://doi.org/10.1002/15-1061.

Berkeley Earth, 2018. Land+Ocean Data. Retrieved from http://berkeleyearth.org/land-and-ocean-data/ (Accessed 14 Dec 2018).

Beule, L., Tantanee, S., 2014. The relationship between diurnal temperature range (DTR) and rainfall over northern Thailand. Adv. Mater. Res. 931–932, 614–618. https://doi.org/10.4028/WWW.SCIENTIFIC.NET/AMR.931-932.614.

Beyaztas, U., Yaseen, Z.M., 2019. Drought interval simulation using functional data analysis. J. Hydrol. 579, 124141 https://doi.org/10.1016/j.jhydrol.2019.124141.

Che Ros, F., Tosaka, H., Sidek, L.M., Basri, H., 2016. Homogeneity and trends in long-term rainfall data, Kelantan River Basin, Malaysia. Int. J. River Basin Manag. 14, 151–163.

Chiew, S.Y., Selaman, O.S., Afshar, N.R., 2013. A study on the relationship between climate change and peak discharge in Sarawak river basin. J. Civ. Eng. Sci. Technol. 4, 23–28. https://doi.org/10.33736/JCEST.123.2013.

Cobb, A.R., Harvey, C.F., 2019. Scalar simulation and parameterization of water table dynamics in tropical peatlands. Water Resour. Res. 55, 9351–9377. https://doi.org/10.1029/2019WR025411.

Cobb, A.R., Hoyt, A.M., Gandois, L., Eri, J., Dommain, R., Abu Salim, K., Kai, F.M., Haji Su'ut, N.S., Harvey, C.F., 2017. How temporal patterns in rainfall determine the geomorphology and carbon fluxes of tropical peatlands. Proc. Natl. Acad. Sci. U.S.A. 114, E5187–E5196. https://doi.org/10.1073/pnas.1701090114.

Cordano, E., Eccel, E., 2011. RMAWGEN: Multi-Site Auto-Regressive Weather GENerator. R Packag. version 1.
Davidson, E.A., Belk, E., Boone, R.D., 1998. Soil water content and temperature as independent or confounded factors controlling soil respiration in a temperate mixed hardwood forest. Global Change Biol. 4, 217–227. https://doi.org/10.1046/j.1365-2486.1998.00128.x.
De Longueville, F., Hountondji, Y.C., Kindo, I., Gemenne, F., Ozer, P., 2016. Long-term analysis of rainfall and temperature data in Burkina Faso (1950–2013). Int. J. Climatol. 36, 4393–4405. https://doi.org/10.1002/JOC.4640.
Decker, M., Brunke, M.A., Wang, Z., Sakaguchi, K., Zeng, X., Bosilovich, M.G., 2012. Evaluation of the reanalysis products from GSFC, NCEP, and ECMWF using flux tower observations. J. Clim. 25, 1916–1944. https://doi.org/10.1175/jcli-d-11-00004.1.
Di Cecco, G.J., Gouhier, T.C., 2018. Increased spatial and temporal autocorrelation of temperature under climate change. Sci. Rep. 81 (8), 1–9. https://doi.org/10.1038/s41598-018-33217-0, 2018.
Dindang, A., Taat, A., Beng, P.E., Alwi, A.M., Mandai, A., Adam, S.M., Othman, F., Bima, D.A., Lah, D., 2013. Statistical and trend analysis of rainfall data in Kuching, Sarawak from 1968–2010. JMM Res. Publ. 6, 17.
Diong, J.Y., Yip, W.S., MatAdam, M.K., Chang, N.K., Yunus, F., Abdullah, M.H., 2015. The definitions of the southwest monsoon climatological onset and withdrawal over Malaysian region. Malaysian Meteorol. Dep. 3, 1–30.
Dohong, A., Aziz, A.A., Dargusch, P., 2017. A review of the drivers of tropical peatland degradation in South-East Asia. Land Use Pol. 69, 349–360. https://doi.org/10.1016/j.landusepol.2017.09.035.
Dommain, R., Cobb, A.R., Joosten, H., Glaser, P.H., Chua, A.F.L., Gandois, L., Kai, F.M., Noren, A., Salim, K.A., Su'ut, N.S.H., Harvey, C.F., 2015. Forest dynamics and tip-up pools drive pulses of high carbon accumulation rates in a tropical peat dome in Borneo (Southeast Asia). J. Geophys. Res. Biogeosciences. https://doi.org/10.1002/2014JG002796.
Donat, M.G., Alexander, L.V., Yang, H., Durre, I., Vose, R., Dunn, R.J.H., Willett, K.M., Aguilar, E., Brunet, M., Caesar, J., Hewitson, B., Jack, C., Klein Tank, A.M.G., Kruger, A.C., Marengo, J., Peterson, T.C., Renom, M., Oria Rojas, C., Rusticucci, M., Salinger, J., Elrayah, A.S., Sekele, S.S., Srivastava, A.K., Trewin, B., Villarroel, C., Vincent, L.A., Zhai, P., Zhang, X., Kitching, S., 2013. Updated analyses of temperature and precipitation extreme indices since the beginning of the twentieth century: the HadEX2 dataset. J. Geophys. Res. Atmos. 118, 2098–2118. https://doi.org/10.1002/jgrd.50150.
Ehsanzadeh, E., Adamowski, K., 2010. Trends in timing of low stream flows in Canada: impact of autocorrelation and long-term persistence. Hydrol. Process. An Int. J. 24, 970–980.
Fathian, F., Morid, S., Kahya, E., 2014. Identification of trends in hydrological and climatic variables in Urmia Lake basin, Iran. Theor. Appl. Climatol. 119, 443–464. https://doi.org/10.1007/s00704-014-1120-4.
Feher, L.C., Osland, M.J., Griffith, K.T., Grace, J.B., Howard, R.J., Stagg, C.L., Enwright, N.M., Krauss, K.W., Gabler, C.A., Day, R.H., Rogers, K., 2017. Linear and nonlinear effects of temperature and precipitation on ecosystem properties in tidal saline wetlands. Ecosphere 8, e01956. https://doi.org/10.1002/ecs2.1956.
Ferrari, G.T., Ozaki, V., 2014. Missing data imputation of climate datasets: implications to modeling extreme drought events. Rev. Bras. Meteorol. 29, 21–28. https://doi.org/10.1590/s0102-77862014000100003.
Frich, P., Alexander, L.V., Della-Marta, P., Gleason, B., Haylock, M., Klein Tank, A.M.G., Peterson, T., 2002. Observed coherent changes in climatic extremes during the second half of the twentieth century. Clim. Res. 19, 193–212. https://doi.org/10.3354/cr019193.
Fung, K.F., Chew, K.S., Huang, Y.F., Ahmed, A.N., Teo, F.Y., Ng, J.L., Elshafie, A., 2022. Evaluation of spatial interpolation methods and spatiotemporal modeling of rainfall distribution in Peninsular Malaysia. Ain Shams Eng. J. 13, 101571 https://doi.org/10.1016/J.ASEJ.2021.09.001.
Ge, F., Zhu, S., Peng, T., Zhao, Y., Sielmann, F., Fraedrich, K., Zhi, X., Liu, X., Tang, W., Ji, L., 2019. Risks of precipitation extremes over Southeast Asia: does 1.5 °C or 2 °C global warming make a difference? Environ. Res. Lett. 14, 44015 https://doi.org/10.1088/1748-9326/AAFF7E.
Gomyo, M., Kuraji, K., 2009. Spatial and temporal variations in rainfall and the ENSO-rainfall relationship over Sarawak, Malaysian Borneo. SOLA 5, 41–44. https://doi.org/10.2151/sola.2009-011.
Gordon, A.L., Huber, B.A., Metzger, E.J., Susanto, R.D., Hurlburt, H.E., Adi, T.R., 2012. South China Sea throughflow impact on the Indonesian throughflow. Geophys. Res. Lett. 39 https://doi.org/10.1029/2012gl052021.
Halder, B., Ameen, A.M.S., Bandyopadhyay, J., Khedher, K.M., Yaseen, Z.M., 2022. The impact of climate change on land degradation along with shoreline migration in Ghoramara Island, India. Phys. Chem. Earth, Parts A/B/C 126, 103135.
Halder, B., Haghbin, M., Farooque, A.A., 2021. An assessment of urban expansion impacts on land transformation of rajpur-sonarpur municipality. Knowledge-Based Eng. Sci. 2, 34–53.
Hamed, K.H., 2009. Exact distribution of the Mann–Kendall trend test statistic for persistent data. J. Hydrol. 365, 86–94. https://doi.org/10.1016/j.jhydrol.2008.11.024.
Hamed, K.H., 2008. Trend detection in hydrologic data: the Mann-Kendall trend test under the scaling hypothesis. J. Hydrol. 349, 350–363. https://doi.org/10.1016/j.jhydrol.2007.11.009.
Hanif, M.F., Mustafa, M.R.U., Liaqat, M.U., Hashim, A.M., Yusof, K.W., 2022. Evaluation of long-term trends of rainfall in perak, Malaysia. Clim. Past 2022, 44. https://doi.org/10.3390/CLI10030044, 10, Page 44 10.
Harris, I., Jones, P.D., Osborn, T.J., Lister, D.H., 2013. Updated High-Resolution Grids of Monthly Climatic Observations – the CRU TS3 . 10 Dataset. https://doi.org/10.1002/joc.3711.
Harrison, R.D., n.d. , 2005, A Severe Drought in Lambir Hills National Park. Pollinat. Ecol. Rain For. https://doi.org/10.1007/0-387-27161-9_5,.
Hasan, H., Hanim, N., Salleh, M., 2016. Climate change risk reduction through readiness: an assessment of extreme temperature indices for Peninsular Malaysia. Geogr. – Malaysian J. Soc. Sp. 12, 10–20.
He, Y., Lin, K., Tang, G., Chen, X., Guo, S., Gui, F., 2017. Quantifying the changing properties of climate extremes in Guangdong Province using individual and integrated climate indices. Int. J. Climatol. 37, 781–792. https://doi.org/10.1002/JOC.4739.
Hikouei, I.S., Eshleman, K.N., Saharjo, B.H., Graham, L.L.B., Applegate, G., Cochrane, M. A., 2023. Using machine learning algorithms to predict groundwater levels in Indonesian tropical peatlands. Sci. Total Environ. 857, 159701 https://doi.org/10.1016/J.SCITOTENV.2022.159701.
Hin, C., Bong, J., Putuhena, F.J., Bong, C., Joo, H., Sie Yew, T., Bustami, R.A., 2009. Impact of climate change and its variability on the rainfall pattern in Sarawak river basin. In: International Conference on Water Resources. ICWR, pp. 26–27, 2009.
Huffman, G.J., Bolvin, D.T., Nelkin, E.J., 2015. Integrated multi-satellitE retrievals for GPM (IMERG) technical documentation. NASA/GSFC Code 612, 47.
Hussain, M., Yusof, K.W., Mustafa, M.R., Afshar, N.R., 2015. Application of statistical downscaling model (SDSM) for long term prediction of rainfall in Sarawak, Malaysia. WIT Trans. Ecol. Environ. 196, 269–278. https://doi.org/10.2495/WRM150231.
Hussain, M., Yusof, K.W., Mustafa, M.R., Mahmood, R., Shaofeng, J., 2017. Projected changes in temperature and precipitation in Sarawak state of Malaysia for selected Cmip5 climate scenarios. Int. J. Sustain. Dev. Plann. 12, 1299–1311. https://doi.org/10.2495/SDP-V12-N8-1299-1311.
Hyndman, R., 2015. Time Series Data Library.
IPCC, 2014. Climate Change 2014: Synthesis Report. Contribution of Working Groups I, II and III to the Fifth Assessment Report of the Intergovernmental Panel on Climate Change. Ipcc.
Iqbal, Z., Shahid, S., Ahmed, K., Ismail, T., Ziarh, G.F., Chung, E.-S., Wang, X., 2021. Evaluation of CMIP6 GCM rainfall in mainland Southeast Asia. Atmos. Res. 254, 105525 https://doi.org/10.1016/j.atmosres.2021.105525.
Ise, T., Dunn, A.L., Wofsy, S.C., Moorcroft, P.R., 2008. High sensitivity of peat decomposition to climate change through water-table feedback. Nat. Geosci. 1, 763–766. https://doi.org/10.1038/ngeo331.
Joseph, B., Bhatt, B.C., Koh, T.Y., Chen, S., 2008. Sea breeze simulation over the Malay Peninsula in an intermonsoon period. J. Geophys. Res. 113 https://doi.org/10.1029/2008jd010319.
Juneng, L., Tangang, F.T., 2005. Evolution of ENSO-related rainfall anomalies in Southeast Asia region and its relationship with atmosphere–ocean variations in Indo-Pacific sector. Clim. Dynam. 25, 337–350. https://doi.org/10.1007/s00382-005-0031-6.
Karl, T.R., Nicholls, N., Ghazi, A., 1999. CLIVAR/GCOS/WMO workshop on indices and indicators for climate extremes workshop summary. Weather Clim. Extrem. https://doi.org/10.1007/978-94-015-9265-9_2.
Katsanos, D., Retalis, A., Tymvios, F., Michaelides, S., 2018. Study of extreme wet and dry periods in Cyprus using climatic indices. Atmos. Res. 208, 88–93. https://doi.org/10.1016/J.ATMOSRES.2017.09.002.
Khan, N., Shahid, S., Ismail, T. bin, Wang, X.-J., 2018. Spatial distribution of unidirectional trends in temperature and temperature extremes in Pakistan. Theor. Appl. Climatol. 136, 899–913. https://doi.org/10.1007/s00704-018-2520-7.
Kim, J.B., Bae, D.H., 2021. The impacts of global warming on climate zone changes over Asia based on CMIP6 projections. Earth Space Sci. 8, e2021EA001701 https://doi.org/10.1029/2021EA001701.
Kottek, M., Grieser, J., Beck, C., Rudolf, B., Rubel, F., 2006. World Map of the Köppen-Geiger climate classification updated. Meteorol. Z. 15, 259–263. https://doi.org/10.1127/0941-2948/2006/0130.
Koutsoyiannis, D., Montanari, A., 2007. Statistical analysis of hydroclimatic time series: uncertainty and insights. Water Resour. Res. 43 https://doi.org/10.1029/2006wr005592.
Kozan, O., 2020. Trend analysis of rainfall characteristics in the kemena and tatau river basins, Sarawak. Adv. Asian Human-Environmental Res. 71–83. https://doi.org/10.1007/978-981-13-7513-2_4.
Kreitmeier, S., Wokaun, A., Büchi, F.N., Watts, J.D., Natali, S.M., Carlson, K.M., Goodman, L.K., May-Tobin, C.C., 2015. Modeling relationships between water table depth and peat soil carbon loss in Southeast Asian plantations. Environ. Res. Lett. 10, 74006 https://doi.org/10.1088/1748-9326/10/7/074006.
Krishnan, M.V.N., Prasanna, M.V., Vijith, H., 2018. Statistical analysis of trends in monthly precipitation at the limbang river basin, Sarawak (NW Borneo), Malaysia. Meteorol. Atmos. Phys. 1314 (131), 883–896. https://doi.org/10.1007/S00703-018-0611-8, 2018.
Kurita, N., Horikawa, M., Kanamori, H., Fujinami, H., Kumagai, T., Kume, T., Yasunari, T., 2018. Interpretation of El Niño–Southern Oscillation-related precipitation anomalies in north-western Borneo using isotopic tracers. Hydrol. Process. 32, 2176–2186. https://doi.org/10.1002/HYP.13164.
Lacombe, G., Hoanh, C.T., Smakhtin, V., 2012. Multi-year variability or unidirectional trends? Mapping long-term precipitation and temperature changes in continental Southeast Asia using PRECIS regional climate model. Clim. Change 113, 285–299. https://doi.org/10.1007/s10584-011-0359-3.
Lacombe, G., McCartney, M., 2014. Uncovering consistencies in Indian rainfall trends observed over the last half century. Clim. Change 123, 287–299. https://doi.org/10.1007/S10584-013-1036-5/FIGURES/3.

Leong Tan, M., Samat, N., Chan, N.W., Lee, A.J., Li, C., 2019. Analysis of Precipitation and Temperature Extremes over the Muda River Basin. https://doi.org/10.3390/w11020283. Malaysia.

Liu, D., Zhao, Q., Guo, S., Liu, P., Xiong, L., Yu, X., Zou, H., Zeng, Y., Wang, Z., 2019. Variability of spatial patterns of autocorrelation and heterogeneity embedded in precipitation. Nord. Hydrol 50, 215–230. https://doi.org/10.2166/NH.2018.054.

Llanos-Herrera, L., 2014. RClim Tool: User Manual and Video.

Longobardi, A., Boulariah, O., 2022. Long-term regional changes in inter-annual precipitation variability in the Campania Region. Southern Italy. Theor. Appl. Climatol. 148, 869–879. https://doi.org/10.1007/S00704-022-03972-2/FIGURES/7.

Mallick, J., Salam, R., Islam, H.M.T., Shahid, S., Kamruzzaman, M., Pal, S.C., Bhat, S.A., Elbeltagi, A., Rodrigues, T.R., Ibrahim, S.M., Islam, A.R.M.T., 2022. Recent changes in temperature extremes in subtropical climate region and the role of large-scale atmospheric oscillation patterns. Theor. Appl. Climatol. 148, 329–347. https://doi.org/10.1007/S00704-021-03914-4/FIGURES/7.

Manton, M.J., Della-Marta, P.M., Haylock, M.R., Hennessy, K.J., Nicholls, N., Chambers, L.E., Collins, D.A., Daw, G., Finet, A., Gunawan, D., Inape, K., Isobe, H., Kestin, T.S., Lefale, P., Leyu, C.H., Lwin, T., Maitrepierre, L., Ouprasitwong, N., Page, C.M., Pahalad, J., Plummer, N., Salinger, M.J., Suppiah, R., Tran, V.L., Trewin, B., Tibig, I., Yee, D., 2001. Trends in extreme daily rainfall and temperature in Southeast Asia and the South pacific: 1961-1998. Int. J. Climatol. 21, 269–284. https://doi.org/10.1002/joc.610.

Matsuura, K., Willmott, C.J., 2012. Terrestrial Precipitation: 1900–2010 Gridded Monthly Time Series (Version 3.02). Cent. Clim. Res. Univ. Delaware, Newark, DE.

Mayowa, O.O., Pour, S.H., Shahid, S., Mohsenipour, M., Harun, S.B.I.N., Heryansyah, A., Ismail, T., 2015. Trends in rainfall and rainfall-related extremes in the east coast of peninsular Malaysia. J. Earth Syst. Sci. 124, 1609–1622. https://doi.org/10.1007/s12040-015-0639-9.

Mckee, T.B., Doesken, N.J., Kleist, J., 1993. The relationship of drought frequency and duration to time scales. AMS 8th Conf. Appl. Climatol. 179–184.

McLeod, A.I., Hipel, K.W., 1978. Preservation of the rescaled adjusted range: 1. A reassessment of the Hurst Phenomenon. Water Resour. Res. 14, 491–508. https://doi.org/10.1029/wr014i003p00491.

Mezbahuddin, S., Nikonovas, T., Spessa, A., Grant, R., Imron, M., 2022. Modelling Large-Scale Seasonal Variations in Water Table Depth over Tropical Peatlands in Riau, Sumatra. Authorea Prepr. https://doi.org/10.1002/ESSOAR.10501280.1.

Miettinen, J., Shi, C., Liew, S.C., 2017. Fire distribution in peninsular Malaysia, Sumatra and Borneo in 2015 with special emphasis on peatland fires. Environ. Manag. 60, 747–757. https://doi.org/10.1007/S00267-017-0911-7/FIGURES/6.

Mishra, A., Liu, S.C., 2014. Changes in precipitation pattern and risk of drought over India in the context of global warming. J. Geophys. Res. Atmos. 119, 7833–7841. https://doi.org/10.1002/2014jd021471.

Najib, M.K., Nurdiati, S., Sopaheluwakan, A., 2022. Copula-based joint distribution analysis of the ENSO effect on the drought indicators over Borneo fire-prone areas. Model. Earth Syst. Environ. 8, 2817–2826. https://doi.org/10.1007/S40808-021-01267-5/FIGURES/5.

Nashwan, M.S., Ismail, T., Ahmed, K., 2019. Non-stationary analysis of extreme rainfall in peninsular Malaysia. J. Sustain. Sci. Manag 14, 17–34.

Nashwan, M.S., Shahid, S., 2019. Spatial distribution of unidirectional trends in climate and weather extremes in Nile river basin. Theor. Appl. Climatol. 137, 1181–1199.

Navidi Nassaj, B., Zohrabi, N., Nikbakht Shahbazi, A., Fathian, H., 2022. Evaluating the performance of eight global gridded precipitation datasets across Iran. Dynam. Atmos. Oceans 98, 101297. https://doi.org/10.1016/J.DYNATMOCE.2022.101297.

Ng, C.Y., Jaafar, W.Z.W., Mei, Y., Othman, F., Lai, S.H., Liew, J., 2022. Assessing the changes of precipitation extremes in peninsular Malaysia. Int. J. Climatol. https://doi.org/10.1002/JOC.7684.

Ngau, L.D., Fong, S.S., Khoon, K.L., Rumpang, E., Vasander, H., Jauhiainen, J., Yrjälä, K., Silvennoinen, H., 2022. Mapping peat soil moisture under oil palm plantation and tropical forest in Sarawak. Mires Peat 28. https://doi.org/10.19189/MAP.2022.OMB.STA.2370.

Noce, S., Caporaso, L., Santini, M., 2020. A new global dataset of bioclimatic indicators. Sci. Data 71 (7), 1–12. https://doi.org/10.1038/s41597-020-00726-5, 2020.

Panda, D.K., Panigrahi, P., Mohanty, S., Mohanty, R.K., Sethi, R.R., 2016. The 20th century transitions in basic and extreme monsoon rainfall indices in India: comparison of the ETCCDI indices. Atmos. Res. 181, 220–235. https://doi.org/10.1016/J.ATMOSRES.2016.07.002.

Peng, S., Huang, J., Sheehy, J.E., Laza, R.C., Visperas, R.M., Zhong, X., Centeno, G.S., Khush, G.S., Cassman, K.G., 2004. Rice yields decline with higher night temperature from global warming. Proc. Natl. Acad. Sci. U.S.A. 101, 9971–9975. https://doi.org/10.1073/pnas.0403720101.

Peterson, T., Folland, C., Gruza, G., Hogg, W., Mokssit, A., Plummer, N., 2001. Report on the Activities of the Working Group on Climate Change Detection and Related Rapporteurs. World Meteorological Organization, Geneva.

Popov, T., Gnjato, S., Trbić, G., Ivanišević, M., 2017. Recent trends in extreme temperature indices in Bosnia and Herzegovina. Carpathian J. Earth Environ. Sci. 13, 211–224. https://doi.org/10.26471/cjees/2018/013/019.

Pour, S.H., Wahab, A.K.A., Shahid, S., 2020. Spatiotemporal changes in aridity and the shift of drylands in Iran. Atmos. Res. https://doi.org/10.1016/j.atmosres.2019.104704.

Qu, M., Wan, J., Hao, X., 2014. Analysis of diurnal air temperature range change in the continental United States. Weather Clim. Extrem. 4, 86–95. https://doi.org/10.1016/J.WACE.2014.05.002.

Rahimi, M., Mohammadian, N., Vanashi, A.R., Whan, K., 2018. Trends in indices of extreme temperature and precipitation in Iran over the period 1960-2014. Open J. Ecol. 396–415. https://doi.org/10.4236/oje.2018.87024, 08.

Rana, S., Deoli, V., Sagar, ·, Chavan, R., 2022. Detection of abrupt change in trends of rainfall and rainy day's pattern of Uttarakhand. Arabian J. Geosci. 157 (15), 1–17. https://doi.org/10.1007/S12517-022-09883-W, 2022.

Rasmusson, E.M., Carpenter, T.H., 1982. Variations in tropical sea surface temperature and surface wind fields associated with the southern oscillation/el Niño. Mon. Weather Rev. 110, 354–384. https://doi.org/10.1175/1520-0493(1982)110<0354:vitsst>2.0.co;2.

Razavi, T., Switzman, H., Arain, A., Coulibaly, P., 2016. Regional climate change trends and uncertainty analysis using extreme indices: a case study of Hamilton, Canada. Clim. Risk Manag. 13, 43–63. https://doi.org/10.1016/j.crm.2016.06.002.

Rienecker, M.M., Suarez, M.J., Gelaro, R., Todling, R., Bacmeister, J., Liu, E., Bosilovich, M.G., Schubert, S.D., Takacs, L., Kim, G.-K., Bloom, S., Chen, J., Collins, D., Conaty, A., da Silva, A., Gu, W., Joiner, J., Koster, R.D., Lucchesi, R., Molod, A., Owens, T., Pawson, S., Pegion, P., Redder, C.R., Reichle, R., Robertson, F. R., Ruddick, A.G., Sienkiewicz, M., Woollen, J., 2011. MERRA: NASA's Modern-Era Retrospective analysis for research and applications. J. Clim. 24, 3624–3648. https://doi.org/10.1175/jcli-d-11-00015.1.

Rousta, I., Doostkamian, M., Haghighi, E., Ghafarian Malamiri, H.R., Yarahmadi, P., 2017. Analysis of spatial autocorrelation patterns of heavy and super-heavy rainfall in Iran. Adv. Atmos. Sci. 349 (34), 1069–1081. https://doi.org/10.1007/S00376-017-6227-Y, 2017.

Sa'adi, Z., Shahid, S., Ismail, T., Chung, E.S., Wang, X.J., 2017. Trends analysis of rainfall and rainfall extremes in Sarawak, Malaysia using modified Mann–Kendall test. Meteorol. Atmos. Phys. https://doi.org/10.1007/s00703-017-0564-3.

Sa'adi, Z., Shahid, S., Shiru, M.S., 2021. Defining climate zone of Borneo based on cluster analysis. Theor. Appl. Climatol. 145, 1467–1484. https://doi.org/10.1007/S00704-021-03701-1/TABLES/2.

Salehie, O., Ismail, T. bin, Shahid, S., Sammen, S.S., Malik, A., Wang, X., 2022. Selection of the gridded temperature dataset for assessment of thermal bioclimatic environmental changes in Amu Darya River basin. Stoch. Environ. Res. Risk Assess. 1–21. https://doi.org/10.1007/S00477-022-02172-8/FIGURES/13.

Salman, S.A., Shahid, S., Sharafati, A., Ahmed Salem, G.S., Abu Bakar, A., Farooque, A. A., Chung, E.-S., Ahmed, Y.A., Mikhail, B., Yaseen, Z.M., 2021. Projection of agricultural water stress for climate change scenarios: a regional case study of Iraq. Agriculture 11, 1288.

Scheffers, B.R., Edwards, D.P., Diesmos, A., Williams, S.E., Evans, T.A., 2014. Microhabitats reduce animal's exposure to climate extremes. Global Change Biol. 20, 495–503. https://doi.org/10.1111/GCB.12439.

Schnider, U., Becker, A., Finger, P., Meyer-Christoffer, A., Rudolf, B., Ziese, M., 2011. GPCC Full Data Reanalysis Version 6.0 at 0.5○: Monthly Land-Surface Precipitation from Rain-Gauges Built on GTS-Based and Historic Data. FD_M_V6_050.

Sen, P.K., 1968. Estimates of the regression coefficient based on kendall's tau. J. Am. Stat. Assoc. 63, 1379–1389. https://doi.org/10.1080/01621459.1968.10480934.

Shahid, S., 2010. Rainfall variability and the trends of wet and dry periods in Bangladesh. Int. J. Climatol. 30, 2299–2313. https://doi.org/10.1002/joc.2053.

Shahid, S., Wang, X.J., Harun, S., 2014. Unidirectional trends in rainfall and temperature of Bangladesh. IAHS-AISH Proc. reports. Copernic GmbH 363, 177–182.

Shamshirband, S., Hashemi, S., Salimi, H., Samadianfard, S., Asadi, E., Shadkani, S., Kargar, K., Mosavi, A., Nabipour, N., Chau, K.W., 2020. Predicting Standardized Streamflow index for hydrological drought using machine learning models. Eng. Appl. Comput. Fluid Mech. https://doi.org/10.1080/19942060.2020.1715844.

Sheffield, J., Goteti, G., Wood, E.F., 2006. Development of a 50-year high-resolution global dataset of meteorological forcings for land surface modeling. J. Clim. https://doi.org/10.1175/JCLI3790.1.

Sheikh, M.M., Manzoor, N., Ashraf, J., Adnan, M., Collins, D., Hameed, S., Manton, M.J., Ahmed, A.U., Baidya, S.K., Borgaonkar, H.P., Islam, N., Jayasinghearachchi, D., Kothawale, D.R., Premalal, K.H.M.S., Revadekar, J.V., Shrestha, M.L., 2015. Trends in extreme daily rainfall and temperature indices over South Asia. Int. J. Climatol. 35, 1625–1637. https://doi.org/10.1002/JOC.4081.

Silins, U., Rothwell, R.L., 1998. Forest peatland drainage and subsidence affect soil water retention and transport properties in an alberta peatland. Soil Sci. Soc. Am. J. 62, 1048–1056. https://doi.org/10.2136/sssaj1998.03615995006200040028x.

Singh, V., Xiaosheng, Q., 2019. Data assimilation for constructing long-term gridded daily rainfall time series over Southeast Asia. Clim. Dynam. 53, 3289–3313. https://doi.org/10.1007/S00382-019-04703-6/FIGURES/14.

Suhaila, J., Yusop, Z., 2018. Trend analysis and change point detection of annual and seasonal temperature series in Peninsular Malaysia. Meteorol. Atmos. Phys. 130, 565–581.

Sun, Q., Miao, C., Duan, Q., 2016. Extreme climate events and agricultural climate indices in China: CMIP5 model evaluation and projections. Int. J. Climatol. 36, 43–61. https://doi.org/10.1002/JOC.4328.

Sun, X., Ren, G., You, Q., Ren, Y., Xu, W., Xue, X., Zhan, Y., Zhang, S., Zhang, P., 2019. Global diurnal temperature range (DTR) changes since 1901. Clim. Dynam. 52, 3343–3356. https://doi.org/10.1007/S00382-018-4329-6/TABLES/3.

Syafrina, A.H., Norzaida, A., Noor Shazwani, O., 2017. Rainfall analysis in the northern region of Peninsular Malaysia. Int. J. Adv. Appl. Sci. 4, 11–16. https://doi.org/10.21833/IJAAS.2017.011.002.

Talbott, L.D., Rahveh, E., Zeiger, E., 2003. Relative humidity is a key factor in the acclimation of the stomatal response to CO2. J. Exp. Bot. 54, 2141–2147. https://doi.org/10.1093/jxb/erg215.

Tan, W.L., Liew, W.S., Ling, L., 2021. Statistical modelling of extreme rainfall in Peninsular Malaysia. ITM Web Conf 36, 01012. https://doi.org/10.1051/ITMCONF/20213601012.

Tangang, F.T., Juneng, L., Ahmad, S., 2006. Trend and interannual variability of temperature in Malaysia: 1961–2002. Theor. Appl. Climatol. 89, 127–141. https://doi.org/10.1007/s00704-006-0263-3.

Tangang, F.T., Juneng, L., Salimun, E., Kwan, M.S., Le Loh, J., 2013. Projected precipitation changes over Malaysia by the end of the 21st century using PRECIS regional climate model. Clim. Chang. Isl. Coast. Vulnerability. https://doi.org/10.1007/978-94-007-6016-5_1.

Tu, S., Xu, J., Xu, F., al -Kug, J.-S., Ham, Y.-G., Lee, J.-Y., Chen, C.-C., Lin, H.-W., Yu, J.-Y., Lo, M.-H., 2016. The 2015 Borneo fires: what have we learned from the 1997 and 2006 El Niños? Environ. Res. Lett. 11, 104003 https://doi.org/10.1088/1748-9326/11/10/104003.

van Huissteden, J., van den Bos, R., Marticorena Alvarez, I., 2006. Modelling the effect of water-table management on CO2 and CH4 fluxes from peat soils. Netherlands J. Geosci. - Geol. en Mijnb. 85, 3–18. https://doi.org/10.1017/s0016774600021399.

Vose, R.S., Applequist, S., Squires, M., Durre, I., Menne, M.J., Williams, C.N., Fenimore, C., Gleason, K., Arndt, D., 2014. Improved historical temperature and precipitation time series for U.S. Climate divisions. J. Appl. Meteorol. Climatol. 53, 1232–1251. https://doi.org/10.1175/jamc-d-13-0248.1.

Wang, X.L., 2008. Accounting for autocorrelation in detecting mean shifts in climate data series using the penalized maximal t or F test. J. Appl. Meteorol. Climatol. 47, 2423–2444. https://doi.org/10.1175/2008JAMC1741.1.

Warburton, M.L., Schulze, R.E., Jewitt, G.P.W., 2010. Confirmation of *ACRU* model results for applications in land use and climate change studies. Hydrol. Earth Syst. Sci. 14, 2399–2414. https://doi.org/10.5194/hess-14-2399-2010.

Yang, Y., Watanabe, M., Li, F., Zhang, J., Zhang, W., Zhai, J., 2005. Factors affecting forest growth and possible effects of climate change in the Taihang Mountains, northern China. For. An Int. J. For. Res. 79, 135–147. https://doi.org/10.1093/forestry/cpi062.

Yaseen, Z.M., Ali, M., Sharafati, A., Al-Ansari, N., Shahid, S., 2021. Forecasting standardized precipitation index using data intelligence models: regional investigation of Bangladesh. Sci. Rep. 11 https://doi.org/10.1038/s41598-021-82977-9.

Yatagai, A., Arakawa, O., Kamiguchi, K., Kawamoto, H., Nodzu, M.I., Hamada, A., 2009. A 44-year daily gridded precipitation dataset for Asia based on a dense network of rain gauges. SOLA 5, 137–140. https://doi.org/10.2151/sola.2009-035.

Yiiong, S.-P., Bundan, N., 2018. A statistical prediction model of river flood. Borneo J. Sci. Technol. 4, 44–50. https://doi.org/10.3570/bjost.2022.4.1-07.

Yin, H., Sun, Y., 2018. Characteristics of extreme temperature and precipitation in China in 2017 based on ETCCDI indices. Adv. Clim. Change Res. 9, 218–226. https://doi.org/10.1016/J.ACCRE.2019.01.001.

Zhang, X., Hegerl, G., Zwiers, F.W., Kenyon, J., 2005. Avoiding inhomogeneity in percentile-based indices of temperature extremes. J. Clim. 18, 1641–1651. https://doi.org/10.1175/jcli3366.1.

Zhang, Y., Shou, W., Maucieri, C., Lin, F., 2021. Rainfall increasing offsets the negative effects of nighttime warming on GHGs and wheat yield in North China Plain. Sci. Rep. 111 (11), 1–10. https://doi.org/10.1038/s41598-021-86034-3, 2021.

Zhao, C., Huang, Y., Li, Z., Chen, M., 2018. Drought monitoring of Southwestern China using insufficient GRACE data for the long-term mean reference frame under global change. J. Clim. https://doi.org/10.1175/JCLI-D-17-0869.1.